

Patch-wise Retrieval: A Bag of Practical Techniques for Instance-level Matching

Wonseok Choi¹ Sohwi Lim² Nam Hyeon-Woo¹ Moon Ye-Bin¹
 Dong-Ju Jeong³ Jinyoung Hwang³ Tae-Hyun Oh²

¹POSTECH ²KAIST ³Samsung Research

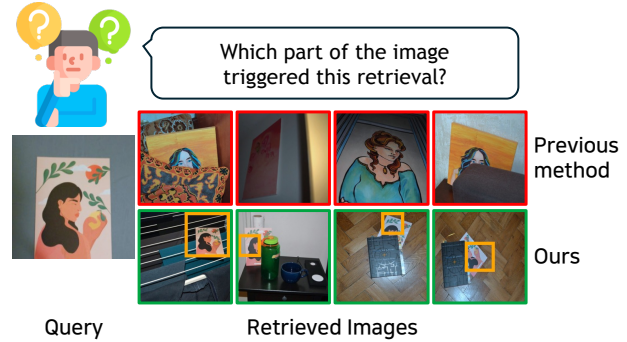
Abstract

Instance-level image retrieval aims to find images containing the same object as a given query, despite variations in size, position, or appearance. To address this challenging task, we propose Patchify, a simple yet effective patch-wise retrieval framework that offers high performance, scalability, and interpretability without requiring fine-tuning. Patchify divides each database image into a small number of structured patches and performs retrieval by comparing these local features with a global query descriptor, enabling accurate and spatially grounded matching. To assess not just retrieval accuracy but also spatial correctness, we introduce LocScore, a localization-aware metric that quantifies whether the retrieved region aligns with the target object. This makes LocScore a valuable diagnostic tool for understanding and improving retrieval behavior. We conduct extensive experiments across multiple benchmarks, backbones, and region selection strategies, showing that Patchify outperforms global methods and complements state-of-the-art reranking pipelines. Furthermore, we apply Product Quantization for efficient large-scale retrieval and highlight the importance of using informative features during compression, which significantly boosts performance. Project website: <https://wons20k.github.io/PatchwiseRetrieval/>

1. Introduction

Instance retrieval is the task of finding images in a database that contain the same visual instance as the one presented in a query image. The target instance may be a specific object, product, person, or landmark, and retrieved images are expected to contain the same object despite variations in perspective, scale, lighting, or background [9, 37]. The task is both practical and broadly applicable, supporting a variety of real-world scenarios [1, 10, 12, 21, 29, 42, 45], such as retrieving relevant personal photos from a user’s device and our daily lives.

Since the appearance of the same instance in a target im-



	Previous method	Ours
Interpretability	✗	✓
Performance	✗	✓
Scalability	✗	✓

Figure 1. **Overview of our patch-wise retrieval framework.** Given a query image, global methods [14, 23, 44] often retrieve visually similar images without indicating what triggered the match. Our approach retrieves correct instances with spatial interpretability by identifying the most relevant regions. Despite using far fewer patches than conventional local feature methods, it achieves strong performance and high scalability.

age, including variations in position, scale, or orientation, instance retrieval requires more discriminative and robust feature representations. To improve instance retrieval under challenging conditions, recent methods [14, 32] have adopted two main strategies: fine-tuning large encoders on domain-specific datasets or employing reranking pipelines with hundreds of dense local descriptors per image. While these approaches offer high accuracy, they introduce practical limitations. Acquiring large-scale instance-level annotations for fine-tuning is often infeasible, and maintaining dense local features per image significantly increases memory and computational overhead. Efficient alternatives that achieve strong performance without fine-tuning or dense local matching remain underexplored.

In this work, we propose **Patchify**, a simple yet effective patch-wise retrieval pipeline that requires only a hand-

ful of local features per image. By leveraging multi-scale grid patches with pretrained visual encoders, Patchify enables efficient, interpretable, and accurate retrieval.

To validate our approach, we conduct a series of experiments evaluating the impact of local features across various settings. We show that patch-wise representations consistently outperform global descriptors, especially with models pretrained on large-scale datasets. We also compare different region sampling strategies, SOTA local feature methods, and find that our simple grid-based Patchify method achieves competitive performance with more complex alternatives. Finally, we apply product quantization for scalable retrieval and observe that training PQ with informative patches, such as those aligned with ground-truth regions, further improves accuracy.

We summarize our main contributions as follows:

- We present Patchify retrieval pipeline, a simple yet effective patch-wise retrieval framework based on multi-scale patch matching that operates without fine-tuning or region proposals.
- We introduce LocScore, a localization-aware metric that provides a fine-grained evaluation of both retrieval accuracy and spatial alignment.
- We conduct extensive experiments across diverse backbones and region sampling strategies, and show that our method offers competitive performance with greater simplicity and interoperability.
- We demonstrate that combining local features with product quantization enables scalable retrieval, and find that using informative patches for PQ training further boosts accuracy.

2. Related work

Instance Level Image Retrieval Methods Early studies in instance level image retrieval relied on hand crafted descriptors such as SIFT [20] and SURF [2]. These approaches extract sparse local keypoints and measure similarity with Bag of Words and geometric verification.

With deep learning, the field moved to dense global CNN descriptors, where pooling schemes such as GeM [25] became dominant and global aggregation methods strengthened robustness [6, 28, 36]. Large-scale pre-training further produced strong global descriptors [3, 8, 26] that transfer across classification, segmentation and retrieval [5, 17, 22, 24, 27, 46]. Nevertheless these global representations can overlook local evidence that discriminates the target instance when it is small, occluded, or away from the image center.

To recover local cues, two-stage pipelines typically perform retrieval with global descriptors and then rerank top candidates using local evidence. A common template compares sets of local descriptors among shortlisted images and promotes those with consistent correspondences, using

attention-based matching, correlation agreement, or structural self-similarity [15, 16, 34].

However, at large scale, storing local descriptors for every database image is prohibitive in memory, and extracting them on demand for each candidate introduces substantial latency. As a result, most approaches confine local processing to a limited first-stage shortlist. Recent work explores how to scale correspondence reasoning under such constraints. For example, long-context sequence modeling enables reasoning over many local descriptors within a single model invocation [39].

In parallel, AMES proposes an efficient asymmetric similarity estimator that achieves practical memory usage and serves as a strong baseline within the ILIAS large-scale evaluation protocol [14, 32]. Despite these advances, much of the existing literature is developed and evaluated primarily on landmark-centric datasets. This setting motivates approaches that generalize beyond landmarks while preserving the complementary strengths of global and local representations. Along this direction, UnED targets general-purpose instance retrieval by adapting modern backbones through simple linear transformations, and the ILIAS protocol demonstrates that such adaptation transfers effectively beyond landmark domains [14, 41].

Patchify densely samples small sliding windows across scales together with a full image patch, embeds them with a frozen backbone, and scores each database image by its best matching patch. This recovers local evidence that global-only descriptors miss on small or off-center targets and avoids the detector dependence of sparse keypoint or proposal methods. Unlike reranking, which needs hundreds of local descriptors per image and therefore computes or stores them only for a shortlist, Patchify indexes a small fixed set per image, so a handful of features provide local signal in the first pass with predictable memory and latency. It requires no training, works plug and play with newer backbones, and, with product quantization, keeps storage close to global baselines while preserving clear spatial attribution.

Explainability via Localization Cues Several retrieval works sought to recover localization cues while keeping a single global descriptor. Integral max pooling builds one global vector and then searches rectangular windows on the feature map of each candidate image using integral images and a generalized mean to approximate channel-wise max pooling [36]. Deep image retrieval learns region-pooled features but aggregates them into one vector for scoring [6]. Because multiple regions are fused into a single representation, the rank signal may not identify an exact region, and localization is obtained only after retrieval, which can dilute fine evidence relative to using explicit localized cues.

Patchify is explainable by design. Each database image is indexed by a small set of multi-scale grid patches, and

the query is compared directly to these regional descriptors, so every match is attributed to a concrete patch. We also introduce LocScore, which combines retrieval rank with intersection over union between the winning patch and the ground truth region to measure alignment and retrieval quality together. We report continuous, mean, and thresholded forms to serve different robustness needs. In contrast to global aggregation, Patchify provides an explicit link from score to region while preserving strong retrieval accuracy.

3. Method

Our goal is to design an instance-level image retrieval framework that is both accurate and interpretable, while maintaining efficiency in terms of computation and memory. To this end, we propose **Patchify**, a single-stage retrieval pipeline that matches structured, non-overlapping patches between query and database images, enabling spatial alignment and interpretability. We also introduce **LocScore**, a localization-aware metric that evaluates whether retrievals are based on the correct image regions. In the following sections, we describe the Patchify pipeline (Sec. 3.1), the LocScore metric for evaluating spatial alignment (Sec. 3.2).

3.1. Patchify: Patch-wise Retrieval pipeline

Our method, Patchify, introduces a simple and efficient way to integrate local spatial cues into instance-level image retrieval without relying on complex region proposals. As illustrated in Figure 2, we divide each database image into a set of structured, non-overlapping grid patches at multiple scales. For example, the L2 configuration includes all patches from the 1×1 , 2×2 , and 3×3 grids, forming a cumulative multi-scale representation. Similarly, L0 uses only a single global 1×1 patch, while L3 further adds 4×4 grid patches on top of L2, providing finer spatial coverage. Each patch is independently encoded using a frozen image encoder (e.g., CLIP, DINOv2), resulting in a compact set of local descriptors per image.

During retrieval, the query image is encoded as a single global descriptor, following standard practice for scalability. We then compute the similarity between this query descriptor and all patch-level descriptors from each database image. For each image, the patch with the highest similarity score is selected to represent its relevance to the query. The final ranking is determined by sorting all database images based on these max similarity scores.

Compared to conventional two-stage retrieval pipelines that rely on hundreds of local features per image and expensive cross-feature comparisons, Patchify uses only a small number of structured patches, leading to significant reductions in both memory and computation. To further enhance efficiency, we apply Product Quantization [11] to compress the patch descriptors and enable fast approximate nearest

neighbor search. Although the method is simple, it achieves strong performance and additionally provides spatial interpretability, as it clearly indicates which specific patch contributed to the retrieval result. This interpretable design not only enhances transparency in retrieval but also enables diagnostic evaluation through LocScore, which quantifies how well the retrieved region aligns with the target object.

3.2. LocScore: Localization-aware Metrics

To evaluate the effectiveness of local features in instance retrieval, we introduce a localization-aware metric, LocScore, which quantifies not only whether the correct image is retrieved, but also how accurately the retrieved region aligns with the target object. Given a query image, the system returns a ranked list of retrieved images along with their most similar local patch.

To reflect not just the presence of correct retrievals but also their order in the ranked list, we weight each prediction by its retrieval precision. This allows us to evaluate localization performance in a retrieval-aware manner, rewarding predictions that are both accurate and highly ranked.

Let $B_{\text{gt}}^{n,i}$ and $B_{\text{pred}}^{n,i}$ denote the ground-truth and predicted bounding boxes, respectively, for the i -th ground-truth image of the n -th query. Suppose this ground-truth image is retrieved at rank $r^{n,i}$, and let $h^{n,i}$ denote the number of ground-truth positives retrieved within the top- $r^{n,i}$ positions.

We first define the localization score for a single query n as:

$$\text{LocScore}^{(n)} = \frac{1}{I_n} \sum_{i=1}^{I_n} \frac{h^{n,i}}{r^{n,i}} \cdot \text{IoU}(B_{\text{gt}}^{n,i}, B_{\text{pred}}^{n,i}), \quad (1)$$

where I_n is the number of ground-truth positives for query n . If a ground-truth image is not retrieved for a given query, its IoU is treated as zero.

The overall LocScore across all queries is then computed by averaging the per-query scores:

$$\text{LocScore} = \frac{1}{N} \sum_{n=1}^N \text{LocScore}^{(n)}, \quad (2)$$

where N is the total number of queries.

We further introduce a thresholded variant of the metric to provide a binary notion of successful localization. While the original formulation captures the degree of spatial alignment through continuous IoU values, this version evaluates whether the predicted region satisfies a minimum localization quality. Specifically, only matches whose IoU exceeds a specified threshold δ are considered correct:

$$\text{LocScore}^{(n)}(\delta) = \frac{1}{I_n} \sum_{i=1}^{I_n} \frac{h^{n,i}}{r^{n,i}} \cdot \mathbb{I} \left[\text{IoU}(B_{\text{gt}}^{n,i}, B_{\text{pred}}^{n,i}) \geq \delta \right], \quad (3)$$

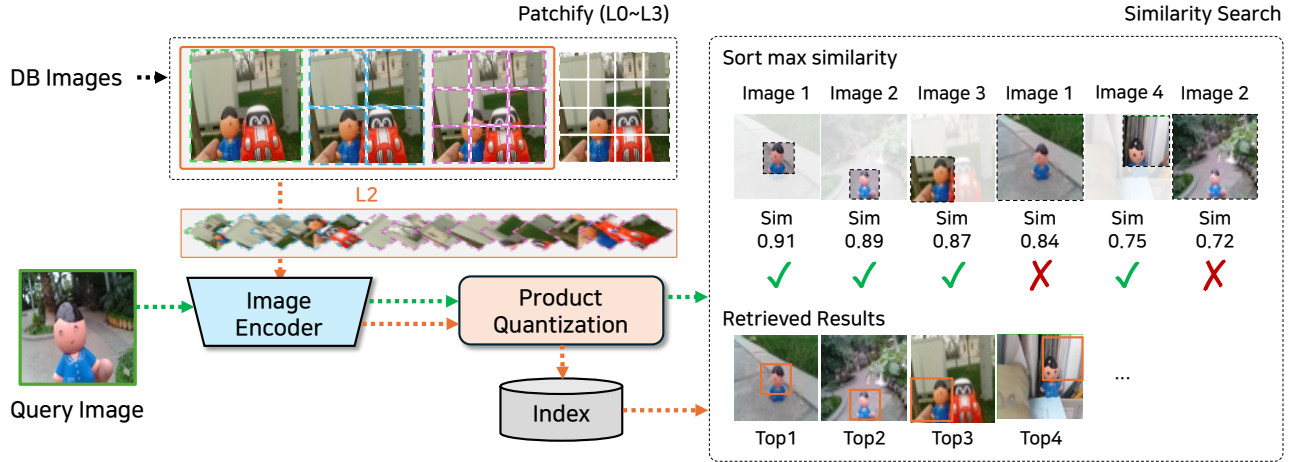


Figure 2. **Overview of our Patchify retrieval pipeline.** We illustrate the L2 configuration, where multi-scale grid patches (1×1 , 2×2 , and 3×3) are extracted and individually passed through the image encoder for feature extraction and indexing. On the right, we show how retrieval is performed for a query: patch-level similarities are computed across the database, and each image is ranked based on the highest-scoring patch it contains.

$$\text{LocScore}(\delta) = \frac{1}{N} \sum_{n=1}^N \text{LocScore}^{(n)}(\delta), \quad (4)$$

where $\mathbb{I}[\cdot]$ is the indicator function.

To reduce sensitivity to the choice of threshold δ , we average over a set of thresholds \mathcal{T} :

$$\text{mLocScore} = \frac{1}{|\mathcal{T}|} \sum_{\delta \in \mathcal{T}} \text{LocScore}(\delta), \quad (5)$$

where $\mathcal{T} = \{0.3, 0.4, 0.5\}$ in our experiments.

This formulation enables both fine-grained and thresholded interpretations of localization performance. Our proposed metrics evaluate two critical aspects: whether the correct image is retrieved, and whether the retrieval is based on the correct local region. Even when the correct image is retrieved, a low LocScore indicates that the retrieval relied on spatially irrelevant content. This makes LocScore a powerful and interpretable diagnostic tool, akin to class activation maps (CAM) in explainable AI.

4. Experiment

We evaluate our Patchify method (Figure 2) on two standard instance retrieval benchmarks, INSTRE [38] and ILIAS core set [14] for most of the comparison, reporting both mean Average Precision (mAP) and our localization-aware metric, LocScore, which reflects retrieval accuracy and spatial alignment. In the main paper, we present results using the continuous LocScore formulation, and provide analyses with thresholded variants in the Supplementary Material (Section S7).

4.1. Effectiveness of Patch-wise Representation

We compare Patchify-based local representations with conventional global descriptors to understand their relative effectiveness in instance-level retrieval. For this experiment, We adopt two widely used pretrained encoders, DINOv2 [23] and CLIP [8], to compare global and local features.

Global vs. Local: A Comparative Analysis As summarized in Table 1, local features consistently outperform global ones across different datasets, encoders, and metrics. This highlights the importance of spatial granularity in improving both retrieval performance and localization quality. We observe local features provide a substantial boost, particularly in challenging scenarios such as occluded or off-center objects. To further contextualize these findings, we conduct a complementary study that compares patch-wise and global representations under challenging conditions such as variation in instance size, spatial position, and image lighting. This study identifies which feature type performs better under each condition and clarifies when local features provide meaningful advantages. The full setup and results are provided in the Supplementary Material.

Qualitative result As shown in Figure 3, we compare the retrieved images of the global and local methods. We observe that Patchify can identify small and non-centered objects. These observations indicate that local features play a crucial role in instance retrieval, particularly under diverse visual conditions affecting the target objects.

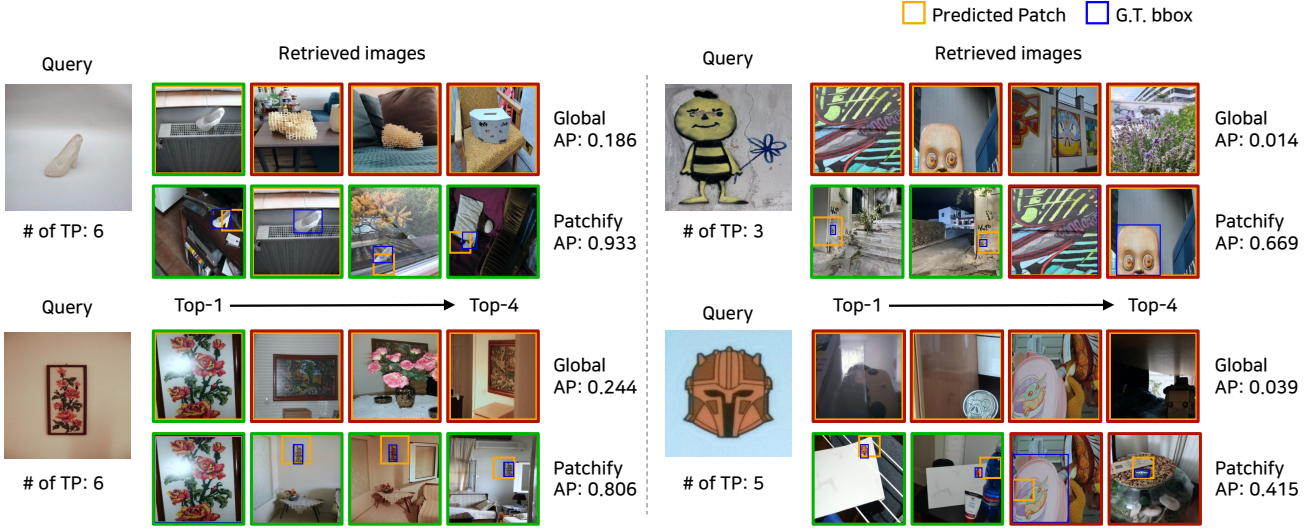


Figure 3. **Qualitative comparison between Global and Patchify on ILIAS.** While global features often fail to retrieve small or non-centered instances, Patchify successfully localizes and retrieves correct instances with better spatial grounding.

Table 1. mAP (%) and LocScore (%) of global and local features on INSTRE and ILIAS. We adopt DINOv2 and CLIP as visual encoders. Using local features are consistently helpful in improving the performance regardless of the kind of visual encoder, dataset, and metrics.

Encoder	Type	INSTRE		ILIAS	
		mAP	LocScore	mAP	LocScore
DINOv2	global	57.70	15.07	40.56	12.18
	local	72.54	22.22	57.52	18.49
CLIP	global	73.84	18.10	31.60	9.18
	local	87.57	30.37	53.35	17.95

Investigation of visual backbone To better understand the impact of model architecture and pretraining data scale on retrieval performance, we conduct a comparative analysis across various visual encoders. Our results indicate that Transformer-based models such as DINOv2, CLIP, and SigLIP consistently outperform CNN-based counterparts, demonstrating the effectiveness of modern architectural designs in both retrieval accuracy and localization quality. Notably, ConvNeXt pretrained on LAION-2B, despite being a CNN, achieves performance on par with Transformer-based models. This observation underscores the importance of large-scale pretraining, which significantly enhances the generalization ability of learned features across architectures. Detailed results can be found in Section S3.

4.2. Interpreting LocScore

In this section, we first compare AP and LocScore and explain how they differ. Next, we present a case study that

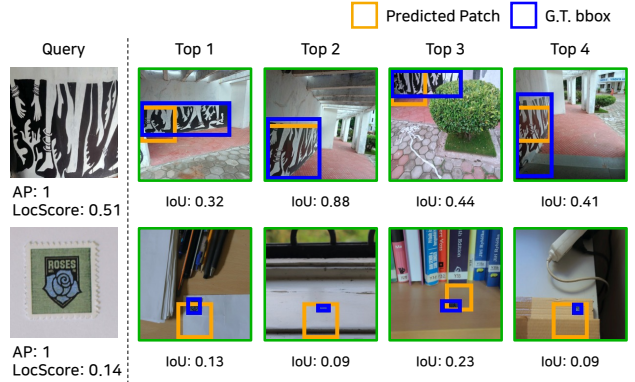


Figure 4. **Comparison of AP and LocScore for evaluating retrieval quality.** Both query examples achieve perfect AP (*i.e.*, all ground-truth images are retrieved), yet their LocScores differ significantly due to localization accuracy. This highlights how LocScore complements AP by incorporating spatial alignment quality.

shows which factors most strongly change LocScore and how rank position and overlap shape the score. Finally, we describe the variants of LocScore and explain when each variant is most appropriate in practice. Due to space limits the detailed discussion of limitations is provided in the Supplementary Material.

AP and LocScore in comparison. In practice, AP can be high while LocScore is low, and this divergence is common when localization is imprecise. Figure 4 shows two queries that both reach AP equal to one, yet their LocScores differ widely. The reason is that AP evaluates ranking only, whereas LocScore couples ranking with spatial alignment

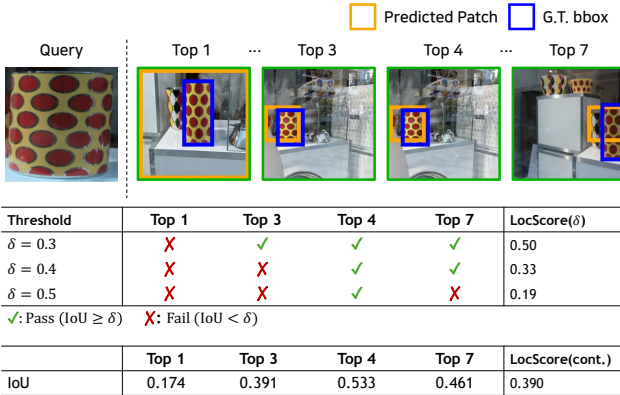


Figure 5. **LocScore variants comparison.** We visualize how the proposed LocScore metric changes as the IoU threshold δ varies and how it is different from the continuous variant. For each threshold, retrieved results are marked as correct if the predicted patch sufficiently overlaps with the ground-truth box ($\text{IoU} \geq \delta$). However, Continuous LocScore strictly evaluates the spatial precision based on IoU.

by multiplying the usual rank contribution with the intersection over union between zero and one. Therefore LocScore is bounded above by AP and it is usually smaller. Moreover LocScore increases only when relevant images appear early and the predicted region on those images has high overlap. If early results align poorly the score remains low even when AP is perfect. When objects are extremely small the grid can cap the attainable overlap, and in that regime, a thresholded variant becomes useful.

Variants of LocScore. Some applications prefer a graded notion of localization, whereas others require a clear pass or fail decision. Figure 5 illustrates the thresholded form. The continuous form weights each positive by its measured overlap and rewards how well the triggering region aligns. In contrast the thresholded form at a chosen delta counts a positive only when the overlap is at least that delta and ignores partial matches. As delta increases, more results fail the test, and the score decreases. When a dataset contains many tiny targets, a small but positive delta, such as 0.09, can better reflect practical acceptability and it can make the two rows in Figure 4 score similarly.

What drives LocScore. Early matches with high overlap lift LocScore more than late, accurate boxes, and patch size and position often limit the attainable overlap. Figure 6 visualizes these effects. The top row gains a higher score because early positives already align well. The middle row ranks competitively, yet the target is large and horizontally elongated, so fixed grid patches cover it poorly, and

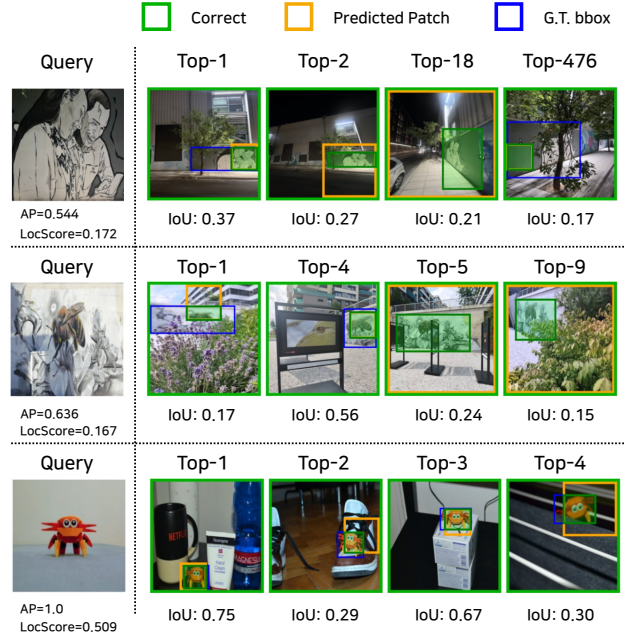


Figure 6. **Case study of LocScore.** Early high-overlap matches raise the score, while late matches or patch granularity limit it.

the score drops. The bottom row shows both strong ranking and reasonable alignment, however the score remains around 0.5 because patch granularity and placement cap the overlap. Therefore, using a finer grid, adding mild overlap between patches, or selecting more suitable regions tends to raise LocScore more effectively than it raises AP. We empirically verify these properties in the following section 4.3.1.

4.3. Method Comparison

In this section, we investigate how different region selection strategies affect instance retrieval performance, and compare our Patchify method against recent state-of-the-art approaches, both as a standalone feature extractor and within reranking pipelines.

Table 2. Comparison of different localization strategies in terms of mAP (%) and LocScore (%) on INSTRE and ILIAS.

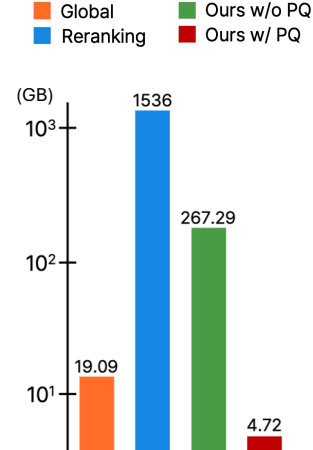
Method	INSTRE		ILIAS	
	mAP	LocScore	mAP	LocScore
Patchify	87.01	24.29	65.16	19.75
Sliding Window (0.5)	89.26	27.50	68.24	22.36
Sliding Window (0.25)	90.62	29.87	70.02	24.57
Region Proposal	92.96	71.44	84.19	68.23

4.3.1. Different region selection strategies

We investigate how different region selection strategies influence instance retrieval, comparing our grid-based

Global feature		Reranking (AMES)	
Method	mAP@1k	Method	mAP@1k
DINOv2 [†]	18.80	DINOv2 [†]	26.50
EVA-CLIP [†]	20.90	OpenCLIP [†]	32.90
MetaCLIP [†]	21.70	SigLIP [†]	40.91
OpenCLIP [†]	22.90	+ Patchify (L3)	48.21
SigLIP2 [†]	37.30	DINOv3	29.86
SigLIP [†]	33.86	+ Patchify (L3)	50.72
+ Patchify (L3)	40.48	SigLIP	26.99
SigLIP	20.41	+ Patchify (L2)	56.54
+ Patchify (L2)	50.27		
DINOv3	21.80		
+ Patchify (L3)	42.98		

(a) Retrieval performance on mini-ILIAS



(b) Memory footprint

Figure 7. **Performance on mini-ILIAS in terms of mAP@1k and DB memory.** A dagger ([†]) denotes the linear adaptation baseline from the ILIAS [14], where the SigLIP encoder is fine-tuned on UnED [40] with a linear probing strategy. Patchify markedly improves over the global baselines, reaching or even surpassing the reranking performance of AMES.

Patchify approach with sliding windows and region proposal methods using strong encoders such as SigLIP.

This analysis provides a comprehensive perspective on how various region-level sampling strategies influence instance retrieval performance. By examining the trade-offs between spatial structure, semantic precision, and coverage, we aim to reveal the strengths and limitations of simple grid-based methods in comparison to more fine-grained or learned approaches. Detailed descriptions of each approach are provided in Supplementary Material (Section S4).

As shown in Table 2, we observe that sliding window methods outperform Patchify in both mAP and Loc-Score, with the 0.25 stride variant achieving the best results. Overall, higher mAP tends to coincide with higher Loc-Score, indicating a positive correlation between retrieval accuracy and spatial alignment. These trends hold consistently across architectures, where increasing patch granularity enhances performance for both CNNs and Transformers. These consistent patterns suggest that better retrieval models not only retrieve the correct images but also localize the target objects more precisely. However, these benefits come at the cost of additional computation and memory, whereas Patchify maintains competitive performance with much greater efficiency.

4.3.2. Comparison with SOTA Methods

To contextualize the effectiveness of Patchify within the broader instance retrieval landscape, we evaluate it against current state-of-the-art methods on the mini-ILIAS [14], which augments the ILIAS core with hard negatives from YFCC100M [35] and is empirically harder than random distractors [14]. We divide our analysis into two retrieval

settings: single-stage retrieval based on global representations, and two-stage reranking.

Single-Stage Retrieval with Global Representations.

We report results for global feature baselines, SigLIP linear adaptation from the ILIAS paper, and the powerful backbone DINOv3 [30]. For numerical comparison, we cite values trained under the same setting from ILIAS [14], shown above the double rule, while the results below are from our own experiments. As shown in Figure 7 (a), Patchify achieves stronger performance than all the baselines. These findings underscore the strength of our Patchify method, which delivers competitive performance in a fully zero-shot setting without requiring any fine-tuning. Furthermore, the use of a stronger backbone with Patchify leads to additional performance gains, suggesting that our patch-based framework benefits directly from improvements in underlying visual encoders.

Integration into Reranking Frameworks. We further evaluate how Patchify integrates into two-stage retrieval pipelines by combining it with AMES [32], a state-of-the-art reranking method based on local descriptor alignment. In this experiment, we don't consider any other recent reranking baselines since they all rely on first-stage retrieval, which our Patchify can serve as. This comparison allows us to assess whether Patchify can serve not only as a standalone retrieval strategy, but also as an effective feature representation within existing reranking architectures. As shown in Figure 7 (a), Patchify demonstrates strong compatibility with reranking architectures, achieving superior

Table 3. Comparison of mAP (%) performance under different multi-scale levels and PQ usage.

Level	Patchify	PQ	INSTRE		ILIAS	
			mAP	LocScore	mAP	LocScore
L0	✗	✗	78.48	18.92	55.03	14.31
	✗	✓	81.99	19.48	54.97	14.30
L1	✓	✗	83.06	21.72	59.45	16.63
	✓	✓	86.20	22.92	57.37	15.65
L2	✓	✗	85.97	23.89	63.32	18.84
	✓	✓	88.20	25.00	59.28	17.00
L3	✓	✗	87.01	24.29	65.16	19.75
	✓	✓	88.52	25.08	59.96	17.33

performance when integrated into AMES compared to prior state-of-the-art models. These results indicate that Patchify not only excels as a standalone retrieval mechanism but also functions effectively as the first-stage representation in reranking systems. Surprisingly, Patchify markedly improves over the global baselines, reaching or even surpassing the reranking performance.

Memory Footprint. We also compare the memory requirements of Patchify against other baselines. To directly contrast Patchify with reranking methods, we report the storage needed to encode and save the entire database at each stage. Note that for reranking, this does not include the additional storage required for global feature retrieval. As shown in Figure 7 (b), Patchify is far more memory-efficient, using $5.75 \times$ less storage (267 vs. 1536 GB). This indicates that even while storing only a handful of patch descriptors per image, Patchify achieves strong performance, highlighting its effectiveness.

4.4. Applying Compression to Local Features

A well-known limitation of local feature-based retrieval methods is their high memory usage, as they require storing a large number of descriptors per image. Unlike conventional approaches, Patchify uses only a small number of structured patch features per image, significantly reducing the memory and computational burden. To further enhance scalability for large-scale retrieval, we apply Inverted File with Product Quantization (IVFPQ) [11]. For more detailed experimental setup, please see Section S6.

Performance comparison. Table 3 presents the retrieval performance before and after applying PQ. As expected, compressing feature representations with PQ can lead to a slight performance drop due to quantization. This trend is observed on the ILIAS benchmark, where the data scale and difficulty are substantially higher. Interestingly, on the smaller and less challenging INSTRE benchmark, PQ

Table 4. Comparison of mAP (%) performance using different training features for PQ.

Training Feature	L0 (1)	L1 (5)	L2 (14)	L3 (30)	G.T. (1)
mAP (%)	60.19	55.80	55.53	53.13	65.07

even yields performance improvements, potentially due to noise reduction or enhanced centroid generalization. Despite compression, local features with PQ still outperform global features in both benchmarks. These results indicate that local characteristics and PQ offer complementary benefits: delivering strong retrieval accuracy with substantially reduced storage.

Training with Informative Features. Product Quantization (PQ) requires a training phase to learn cluster centroids, and the choice of training features can significantly impact retrieval performance. To explore this, we compare PQ trained with features at different patch levels (L0, L1, L2, L3) and with ground-truth-aligned features cropped from instance bounding boxes. As summarized in Table 4, the highest performance is achieved when PQ is trained on ground-truth features, emphasizing the value of using semantically informative representations. Interestingly, features from intermediate patch levels (L1 and L2) perform worse than L0, likely due to the inclusion of background noise or irrelevant content. These results suggest that tighter spatial alignment during PQ training plays a crucial role, and highlight the importance of effective region selection strategies. This highlights a previously underexplored yet critical aspect of PQ training and may inform more robust design choices in future PQ-based retrieval pipelines. Additional qualitative comparisons and visualizations of PQ training features are provided in Section S6.

5. Conclusion

In this work, we introduced Patchify, a simple yet effective patch-wise retrieval framework that achieves strong performance while maintaining both scalability and interpretability. By decomposing each database image into a small set of structured, multi-scale patches, Patchify enables spatially-aware matching without requiring fine-tuning or region proposals. Our experiments demonstrate that Patchify consistently outperforms global feature baselines, adapts well across a variety of backbones, and integrates seamlessly into existing reranking pipelines. To evaluate the spatial quality of retrievals, we proposed LocScore, a localization-aware metric that captures not only retrieval accuracy but also the alignment between retrieved regions and target objects. This metric provides valuable diagnostic insight into how retrieval decisions are made and helps bridge performance evaluation with model interpretability. Furthermore,

we showed that Patchify is highly scalable through the use of PQ. Our analysis revealed that the choice of training features for PQ has a significant impact on performance. In particular, features that are well-aligned with target objects lead to better compression and retrieval accuracy, highlighting the importance of informative patch selection during index construction. Overall, Patchify offers a practical and interpretable design for instance-level image retrieval, enabling efficient matching with minimal computation and memory overhead. Our findings point toward promising future directions for retrieval systems that combine spatial precision, scalability, and transparency.

Acknowledgment

This work was supported by Electronics and Telecommunications Research Institute (ETRI) grant funded by the Korean government [25ZD1160, Development of ICT Convergence Technology for Daegu-Gyeongbuk Regional Industry], Institute of Information & communications Technology Planning & Evaluation (IITP) grant funded by the Korea government(MSIT) (No. 2022-0-00124, No.RS-2022-II220124, Development of Artificial Intelligence Technology for Self-Improving Competency-Aware Learning Capabilities; No.RS-2023-00225630, Development of Artificial Intelligence for Text-based 3D Movie Generation; No.RS-2019-II191906, Artificial Intelligence Graduate School Program(POSTECH))

References

- [1] Jaehun Bang, Ye-Bin Moon, Tae-Hyun Oh, and Kyungdon Joo. Beyond the highlights: Video retrieval with salient and surrounding contexts. In *WACV*, 2026. 1
- [2] Herbert Bay, Tinne Tuytelaars, and Luc Van Gool. Speeded up robust features. In *ECCV*, 2006. 2
- [3] Mathilde Caron, Hugo Touvron, Ishan Misra, Hervé Jégou, Julien Mairal, Piotr Bojanowski, and Armand Joulin. Emerging properties in self-supervised vision transformers. In *ICCV*, pages 9650–9660, 2021. 2
- [4] Timothée Darcet, Maxime Oquab, Julien Mairal, and Piotr Bojanowski. Vision transformers need registers. In *ICLR*, 2024. 4, 5
- [5] Peng Gao, Shijie Geng, Renrui Zhang, Teli Ma, Rongyao Fang, Yongfeng Zhang, Hongsheng Li, and Yu Qiao. Clip-adapter: Better vision-language models with feature adapters. *IJCV*, 2024. 2
- [6] Albert Gordo, Jon Almazán, Jerome Revaud, and Diane Larlus. Deep image retrieval: Learning global representations for image search. In *ECCV*, 2016. 2
- [7] Kaiming He, Xiangyu Zhang, Shaoqing Ren, and Jian Sun. Deep residual learning for image recognition. In *CVPR*, 2016. 2
- [8] Gabriel Ilharco, Mitchell Wortsman, Ross Wightman, Cade Gordon, Nicholas Carlini, Rohan Taori, Achal Dave, Vaishaal Shankar, Hongseok Namkoong, John Miller, Hanneh Hajishirzi, Ali Farhadi, and Ludwig Schmidt. Openclip, 2021. 2, 4
- [9] Tomas Jenicek and Ondrej Chum. No fear of the dark: Image retrieval under varying illumination conditions. In *ICCV*, 2019. 1
- [10] Kim Jun-Seong, Kim GeonU, Kim Yu-Ji, Yu-Chiang Frank Wang, Jaesung Choe, and Tae-Hyun Oh. Dr. splat: Directly referring 3d gaussian splatting via direct language embedding registration. In *CVPR*, 2025. 1
- [11] Herve Jégou, Matthijs Douze, and Cordelia Schmid. Product quantization for nearest neighbor search. *IEEE TPAMI*, 2011. 3, 8
- [12] Kyeong Seon Kim, Seong-Eun Baek, Jung-Mok Lee, and Tae-Hyun Oh. meol: Training-free instruction-guided multi-modal embedder for vector graphics and image retrieval. In *WACV*, 2026. 1
- [13] Alexander Kirillov, Eric Mintun, Nikhila Ravi, Hanzi Mao, Chloe Rolland, Laura Gustafson, Tete Xiao, Spencer Whitehead, Alexander C. Berg, Wan-Yen Lo, Piotr Dollar, and Ross Girshick. Segment anything. In *ICCV*, 2023. 4
- [14] Giorgos Kordopatis-Zilos, Vladan Stojnic, Anna Manko, Pavel Suma, Nikolaos-Antonios Ypsilantis, Nikos Eftymiadis, Zakaria Laskar, Jiri Matas, Ondrej Chum, and Giorgos Tolias. Ilias: Instance-level image retrieval at scale. In *CVPR*, 2025. 1, 2, 4, 7, 5
- [15] Seongwon Lee, Hongje Seong, Suhyeon Lee, and Euntai Kim. Correlation verification for image retrieval. In *CVPR*, 2022. 2
- [16] Seongwon Lee, Suhyeon Lee, Hongje Seong, and Euntai Kim. Revisiting self-similarity: Structural embedding for image retrieval. In *CVPR*, 2023. 2
- [17] Feng Liang, Bichen Wu, Xiaoliang Dai, Kunpeng Li, Yinan Zhao, Hang Zhang, Peizhao Zhang, Peter Vajda, and Diana Marculescu. Open-vocabulary semantic segmentation with mask-adapted clip. In *CVPR*, 2023. 2
- [18] Shilong Liu, Zhaoyang Zeng, Tianhe Ren, Feng Li, Hao Zhang, Jie Yang, Qing Jiang, Chunyuan Li, Jianwei Yang, Hang Su, Jun Zhu, and Lei Zhang. Grounding DINO: Marrying DINO with grounded pre-training for open-set object detection. In *ECCV*, 2024. 4
- [19] Zhuang Liu, Hanzi Mao, Chao-Yuan Wu, Christoph Feichtenhofer, Trevor Darrell, and Saining Xie. A convnet for the 2020s. In *CVPR*, 2022. 2
- [20] David G. Lowe. Distinctive image features from scale-invariant keypoints. *IJCV*, 60(2):91–110, 2004. 2
- [21] Shiyang Lu, Haonan Chang, Eric Pu Jing, Abdeslam Boularias, and Kostas Bekris. Ovir-3d: Open-vocabulary 3d instance retrieval without training on 3d data. In *Conference on Robot Learning*, 2023. 1
- [22] Huaishao Luo, Lei Ji, Ming Zhong, Yang Chen, Wen Lei, Nan Duan, and Tianrui Li. Clip4clip: An empirical study of clip for end to end video clip retrieval and captioning. *Neurocomput.*, 2022. 2
- [23] Maxime Oquab, Timothée Darcet, Théo Moutakanni, Huy Vo, Marc Szafraniec, Vasil Khalidov, Pierre Fernandez, Daniel Haziza, Francisco Massa, Alaaeldin El-Nouby, et al. Dinov2: Learning robust visual features without supervision. *Transactions on Machine Learning Research*, 2024. 1, 4

[24] Yash Patel, Lluis Gomez, Marçal Rusiñol, Dimosthenis Karatzas, and CV Jawahar. Self-supervised visual representations for cross-modal retrieval. In *Proceedings of the 2019 on International Conference on Multimedia Retrieval*, pages 182–186, 2019. 2

[25] Filip Radenović, Giorgos Tolias, and Ondřej Chum. Fine-tuning cnn image retrieval with no human annotation. *IEEE TPAMI*, 41(7):1655–1668, 2019. 2

[26] Alec Radford, Jong Wook Kim, et al. Learning transferable visual models from natural language supervision. In *ICML*, 2021. 2

[27] Yongming Rao, Wenliang Zhao, Guangyi Chen, Yansong Tang, Zheng Zhu, Guan Huang, Jie Zhou, and Jiwen Lu. Denseclip: Language-guided dense prediction with context-aware prompting. In *CVPR*, 2022. 2

[28] Ali Razavian, Josephine Sullivan, Stefan Carlsson, and Atsuto Maki. Visual instance retrieval with deep convolutional networks. *The Journal of The Institute of Image Information and Television Engineers*, 2019. 2

[29] Taichi Sakaguchi, Akira Taniguchi, Yoshinobu Hagiwara, Lotfi El Hafi, Shoichi Hasegawa, and Tadahiro Taniguchi. Object instance retrieval in assistive robotics: Leveraging fine-tuned simsim with multi-view images based on 3d semantic map. In *2024 IEEE/RSJ International Conference on Intelligent Robots and Systems (IROS)*, 2024. 1

[30] Oriane Siméoni, Huy V. Vo, Maximilian Seitzer, Federico Baldassarre, Maxime Oquab, Cijo Jose, Vasil Khalidov, Marc Szafraniec, Seungeun Yi, Michaël Ramamonjisoa, Francisco Massa, Daniel Haziza, Luca Wehrstedt, Jianyuan Wang, Timothée Darcet, Théo Moutakanni, Leonel Sentana, Claire Roberts, Andrea Vedaldi, Jamie Tolan, John Brandt, Camille Couprie, Julien Mairal, Hervé Jégou, Patrick Labatut, and Piotr Bojanowski. DINOv3, 2025. 7

[31] Karen Simonyan and Andrew Zisserman. Very deep convolutional networks for large-scale image recognition. In *ICLR*, 2015. 2

[32] Pavel Suma, Giorgos Kordopatis-Zilos, Ahmet Iscen, and Giorgos Tolias. Ames: Asymmetric and memory-efficient similarity estimation for instance-level retrieval. In *ECCV*, 2024. 1, 2, 7, 4, 5

[33] Christian Szegedy, Wei Liu, Yangqing Jia, Pierre Sermanet, Scott Reed, Dragomir Anguelov, Dumitru Erhan, Vincent Vanhoucke, and Andrew Rabinovich. Going deeper with convolutions. In *CVPR*, 2015. 2

[34] Fuwen Tan, Jiangbo Yuan, and Vicente Ordonez. Instance-level image retrieval using reranking transformers. In *ICCV*, 2021. 2

[35] Bart Thomee, David A Shamma, Gerald Friedland, Benjamin Elizalde, Karl Ni, Douglas Poland, Damian Borth, and Li-Jia Li. Yfcc100m: The new data in multimedia research. *Communications of the ACM*, 2016. 7

[36] Giorgos Tolias, Ronan Sicre, and Hervé Jégou. Particular object retrieval with integral max-pooling of cnn activations. *CoRR*, 2015. 2

[37] Akihiko Torii, Relja Arandjelović, Josef Sivic, Masatoshi Okutomi, and Tomas Pajdla. 24/7 place recognition by view synthesis. In *CVPR*, 2015. 1

[38] Yang Wang, Sheng Yang, Tianzhu Qi, Alan Yuille, and Hong Tang. Instre: A new benchmark for instance-level object retrieval and recognition. In *ACM MM*, 2015. 4

[39] Zilin Xiao, Pavel Suma, Ayush Sachdeva, Hao-Jen Wang, Giorgos Kordopatis-Zilos, Giorgos Tolias, and Vicente Ordonez. Locore: Image re-ranking with long-context sequence modeling. In *CVPR*, 2025. 2

[40] Nikolaos-Antonios Ypsilantis, Kaifeng Chen, Bingyi Cao, Mário Lipovský, Pelin Dogan-Schönberger, Grzegorz Makosa, Boris Bluntschli, Mojtaba Seyedhosseini, Ondřej Chum, and André Araujo. Towards universal image embeddings: A large-scale dataset and challenge for generic image representations. In *ICCV*, 2023. 7

[41] Nikolaos-Antonios Ypsilantis, Kaifeng Chen, Bingyi Cao, Mário Lipovský, Pelin Dogan-Schönberger, Grzegorz Makosa, Boris Bluntschli, Mojtaba Seyedhosseini, Ondřej Chum, and André Araujo. Towards universal image embeddings: A large-scale dataset and challenge for generic image representations. In *ICCV*, 2023. 2

[42] Jiangbo Yuan, An-Ti Chiang, Wen Tang, and Antonio Haro. eproduct: A million-scale visual search benchmark to address product recognition challenges, 2021. 1

[43] Xiaohua Zhai, Alexander Kolesnikov, Neil Houlsby, and Lucas Beyer. Scaling vision transformers. In *CVPR*, 2022. 2

[44] Xiaohua Zhai, Basil Mustafa, Alexander Kolesnikov, and Lucas Beyer. Sigmoid loss for language image pre-training. In *ICCV*, 2023. 1, 2, 4

[45] Xunlin Zhan, Yangxin Wu, Xiao Dong, Yunchao Wei, Minlong Lu, Xiaokang Yang, and Ming-Ming Cheng. Product1m: Towards weakly supervised instance-level product retrieval via cross-modal pretraining. In *ICCV*, 2021. 1

[46] Jinghao Zhou, Chen Wei, Huiyu Wang, Wei Shen, Cihang Xie, Alan Yuille, and Tao Kong. ibot: Image BERT pre-training with online tokenizer. In *ICLR*, 2022. 2

[47] Kaiyang Zhou, Ziwei Liu, Yu Qiao, Tao Xiang, and Chen Change Loy. Domain generalization: A survey. *IEEE TPAMI*, 2023. 2

Patch-wise Retrieval: A Bag of Practical Techniques for Instance-level Matching

Supplementary Material

S1. Overview

This supplementary material provides additional experiments and implementation details that could not be included in the main paper due to space constraints. Following the structure of the main text, we elaborate on the following aspects:

- **Section S2** explains experimental details on the *Impact of Image Characteristics*, such as instance size, position, and brightness, on retrieval performance.
- **Section S3** expands on the *Investigation of Visual Backbones*, comparing CNN and Transformer encoders and the effect of pretraining dataset size.
- **Section S4** details additional comparisons of *Different Region Selection Strategies*, including Patchify, Sliding Window, and Region Proposal methods.
- **Section S5** provides a deeper dive into our *Comparison with SOTA Methods* in both single-stage and reranking settings.
- **Section S6** includes extended analysis on *Product Quantization*, covering memory efficiency, training feature selection, and compression-performance trade-offs.
- **Section S7** further analyze and report thresholded version and average LocScore.
- **Section S8** shows additional *Qualitative Results* that highlight retrieval accuracy and localization behavior across diverse scenarios.

These materials are intended to support and complement the findings in the main paper, offering deeper insight into our proposed approach and its practical implications.

S2. Impact of Image characteristics

S2.1. Analysis

We investigate the effectiveness of global and local features with respect to three factors: instance size, location, and brightness. The first two factors are directly related to our proposed metrics, LocScore; the last factor is a common challenge in instance retrieval. Figure S1 shows the comparison between local and global features. Overall, we observe that local features generally improve performance, demonstrating robustness under varying image conditions.

As shown in Figure S1a, global features outperform local features when the instance occupies a large portion of the image (rightmost group). However, as the instance size decreases, local features begin to outperform global ones, demonstrating their advantage in small object retrieval. Next, we assess the effect of object location by measuring Euclidean distance between the center of the im-

age and the center of the ground-truth bounding box. As shown in Figure S1b, local features maintain more stable retrieval accuracy as the instance moves away from the center, demonstrating greater robustness to spatial displacement.

Lastly, we analyze the impact of image brightness, quantified as the average L-channel value in the Lab color space. In Figure S1c, both global and local features achieve higher performance on images with medium brightness, while performance drops on very dark or very bright images. Nevertheless, local features consistently outperform global features across all brightness levels, even though the overall trend is similar. For a detailed experimental setup, please refer to Section S2.

S2.2. Experimental Details

We adopt CLIP and DINOv2 as the visual encoder for the evaluation. We compare global and local (L3) features with mAP and LocScore on ILLAS core set.

Object bounding box ratio We sort database images with object size by computing the object bounding box area. Then we divide the total object size values equally into 5 bins. For the evaluation, queries with no true positive images in a specific bin are excluded. Global feature works well in big objects but not in small ones.

Object distance from image center We compute L2 distance between the bounding box and the image center and sort them. Then we divide all values equally into 5 bins. Similarly, queries with no true positive images in a specific bin are excluded. Global features work well when the object is centered and not so well when it is not centered.

Brightness of image Unlike the previous two experiments, the evaluation benchmark datasets did not exhibit a meaningful distribution with respect to brightness. To address this, we applied tone mapping by scaling the L channel in the Lab color space to $0.2\times$, $0.6\times$, $1.0\times$, $1.4\times$, and $1.8\times$ of its original value, creating five brightness-adjusted versions of each dataset. We then measured performance on each transformed set.

S3. Investigation of visual backbone

Recently, many visual encoders have been proposed, and we have to choose which visual encoder we use. In this section, we further explore which visual encoders offer the most effective representations for instance retrieval. We analyze a diverse set of models, including both CNN-based (e.g.,

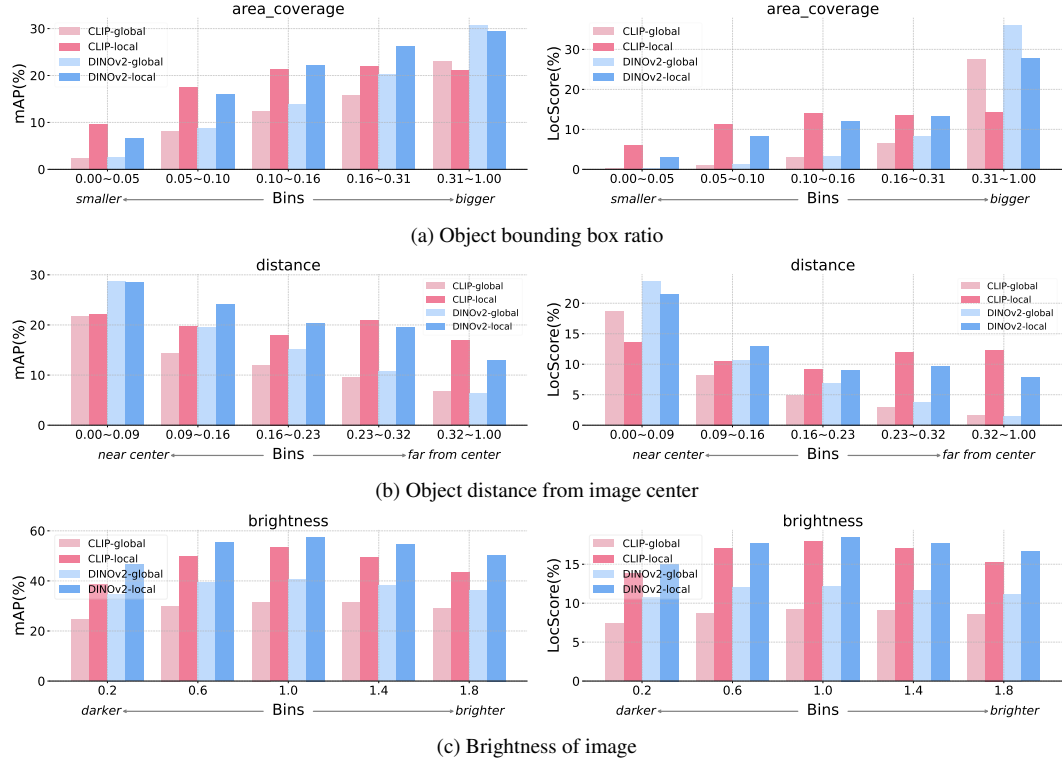


Figure S1. mAP(%) and LocScore(%) of global and local features in terms of object size, distance from image center, and brightness of image. We measure the performance on ILIAS. Both global and local features show a similar trend. In most cases, local features consistently outperform global features across all settings.

VGG [31], ResNet [7], Inception [33], ConvNext [19] and Transformer-based (e.g., DINOv2, CLIP, SigLIP [44]) encoders. This analysis aims to provide deeper insights into the architectural factors that contribute to strong instance-level retrieval performance. Note that we extract local features using Patchify. Throughout all experiments in this paper, unless otherwise specified, we use the Large model configuration and an input image resolution of 384×384 .

Characteristic of visual encoders We compare instance retrieval performance across encoder models with CNN-based and Transformer-based backbones. As shown in Figure S2, based on our analysis using the ILIAS core dataset, as we use more local features, the performance generally increases. ConvNeXt trained on ImageNet is an exceptional case where the performance decreases. Although ConvNeXt pretrained on LAION-2B shows high performance in CNN-based models, transformer-based models generally achieve higher performance compared to CNN-based models.

Impact of pretraining data size of encoder In terms of the exception case of ConvNeXt pretrained on LAION-2B,

we hypothesize that the size of the dataset used during pre-training plays a significant role. As shown in Table 5 and Figure S3, model performance consistently improves with the scale of training data. Regardless of feature dimensionality, increasing the amount of training data improves generalization performance, which in turn enhances instance retrieval performance. This result indicates that representation generalization is influenced by both model capacity and data scale, consistent with findings in prior work [43, 47], and further confirms that this relationship holds for instance retrieval task as well that such an effect also extends to instance retrieval tasks.

S4. Different region selection strategies

We describe the experimental details for evaluating different region selection strategies. We adopt SigLIP as the visual encoder throughout, and conduct evaluations on both the INSTRE and ILIAS core datasets. The following outlines each strategy illustrated in Figure S4:

Global This method follows the standard global feature approach, where the entire image is passed through the encoder to produce a single feature vector.

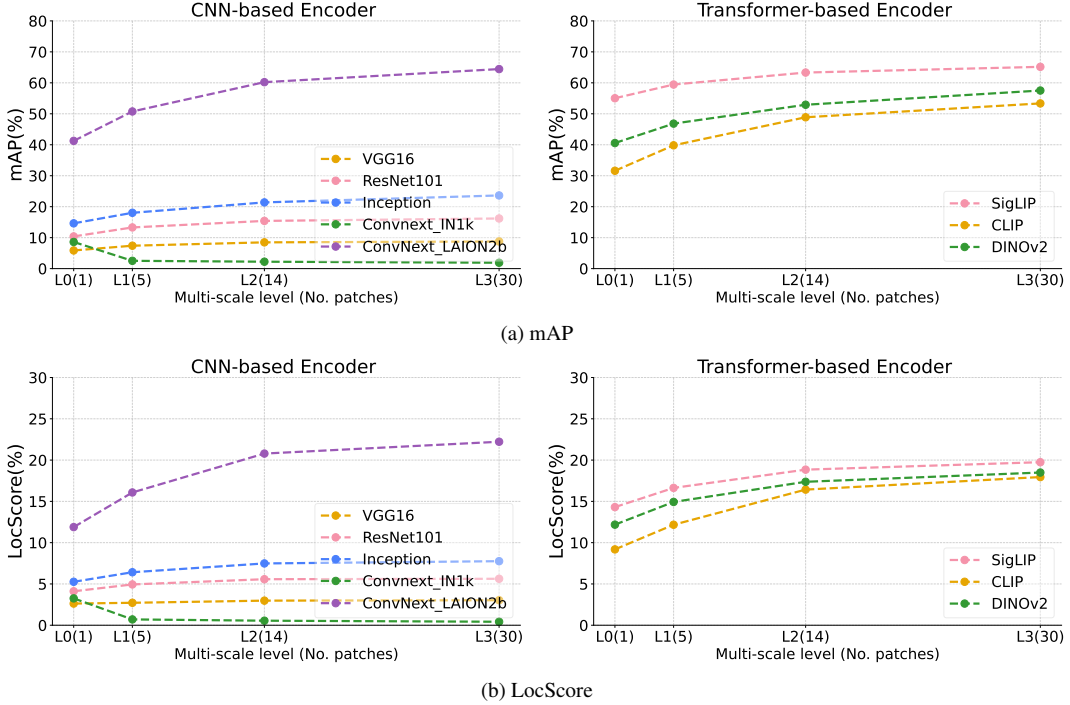


Figure S2. Performance comparison between CNN-based backbone and Transformer-based models based on (a) mAP (%) and (b) LocScore (%) metrics on ILIAS. For comparison, we apply the same scale to plots of CNN-based and Transformer-based models. We observe that transformer-based models show higher performance compared to CNN-based models, except for ConvNext_laion2b.

Table 5. Impact of pretraining data size on instance retrieval performance of encoders.

Dataset (Size)	Encoder (Feat. Dim.)	Type	mAP	
			INSTRE	ILIAS
ImageNet-1K (1M)	VGG16 (4096)	global	26.90	5.86
		local	53.56	8.76
	ResNet101 (2048)	global	36.29	10.40
		local	61.38	16.19
	Inception (1536)	global	27.94	14.62
LVD-142M (142M)	ConvNext (1024)	global	38.97	8.61
		local	56.25	1.90
	DINOv2 (1024)	global	57.70	40.56
		local	72.54	57.51
	CLIP (768)	global	73.83	31.60
LAION-400M (400M)	ConvNext (768)	global	77.95	41.25
		local	92.87	64.44
	SigLIP (1024)	global	78.48	55.03
		local	87.01	65.16

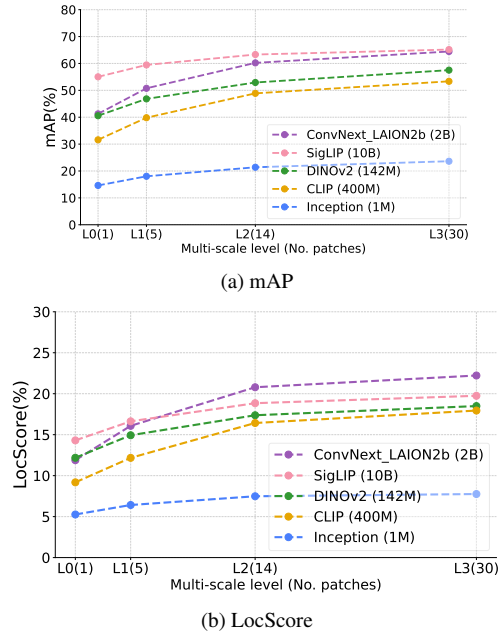


Figure S3. Performance comparison on ILIAS under varying pre-training data sizes. We observe that performance is low if the amount of pre-training data is not sufficient.

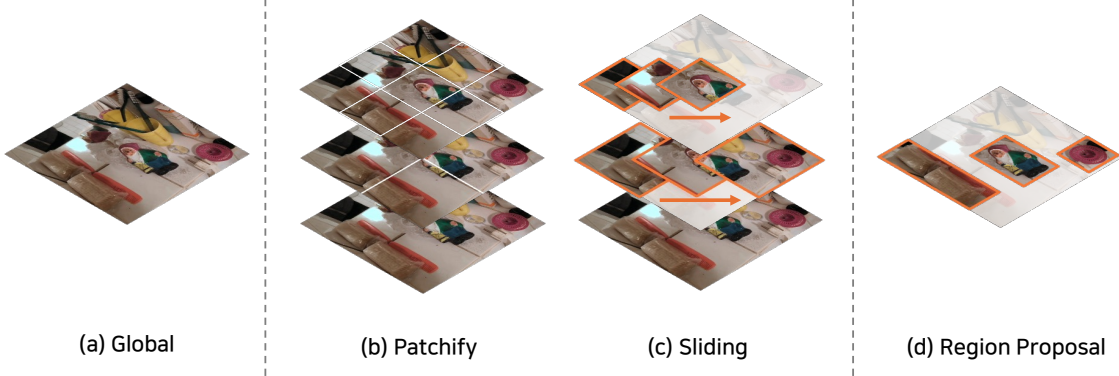


Figure S4. Methods used in analysis. In Global, we use only one embedding. In Patchify, the local features are extracted from the patches of an image. Sliding is similar to Patchify, but the patches have overlap. In Region Proposal, the detector is used to find the informative object in an image and extract the local features by cropping the object.

Patchify This is our proposed method. The image is divided into non-overlapping grid patches according to a pre-defined configuration (e.g., L0, L1, etc.). Each patch is independently passed through the image encoder to extract local descriptors. L0 corresponds to a single 1×1 patch (i.e., the global setting), L1 includes both 1×1 and 2×2 patches, L2 adds 3×3 patches on top of L1, and L3 further includes 4×4 patches. This cumulative multi-scale design allows for spatial interpretability, as the most similar patch can be traced back to a specific region in the image, revealing which part contributed most to the retrieval.

Sliding To assess whether denser and more exhaustive spatial coverage can improve performance, we implement a sliding window approach on the Patchify setting with two different strides: 0.5 and 0.25 relative to the patch size. Unlike Patchify, the sliding window method introduces overlapping patches for denser spatial coverage. This allows us to assess how performance changes as spatial precision improves due to denser sampling. Unlike naive patchify with a grid-based approach, this method produces overlapping patches, potentially increasing the likelihood of including a well-localized region. The goal is to evaluate whether finer sampling improves retrieval accuracy through better spatial alignment.

Region Proposal We further evaluate a more semantically aware region extraction method using Grounding DINO [18], a recent region proposal network capable of producing high-quality object-level bounding boxes. We extract up to 20 bounding boxes per image with a fixed text prompt "object" and use output bounding boxes as regions for feature extraction. Since these proposals are semantically meaningful and often closely aligned with ground-truth objects, this setting allows us to assess the potential upper bound of retrieval performance when informative and well-localized regions are used. Note that the use

Table 6. Comparison with SOTA methods on ILIAS core. Patchify achieves competitive performance as a single-stage method and further boosts performance when integrated into reranking pipelines.

Setting	Feature Extraction Method	mAP (%)
Single-stage	SigLIP (Linear Adaptation) [14]	63.96
	Patchify (SigLIP [44])	65.16
Two-stage	DINOv2 w/ registers [4]	63.37
	SigLIP [14]	75.61
	Patchify (SigLIP [44])	79.54
	Patchify (SigLIP, Linear Adaptation [14])	83.52

of region proposal method for our method is not limited to only Grounding DINO. If any of methods that can produce meaningful and tight region can be used. For example, Segment Anything [13]. Our method can benefit from producing object-aligned patches and informative positives for PQ training, which aligns with our finding that PQ benefits from informative patches.

S5. Comparison with SOTA Methods

In this section, we describe the implementation details for the experiments conducted in Section 4.3.2. Furthermore we also report retrieval performance is measured on ILIAS core set [14], which was not reported in the main paper.

S5.1. Implementation details

AMES For AMES [32], we adopt its asymmetric transformer-based reranking method. During inference, the top- m images retrieved using global similarity are reranked based on local similarities computed via transformer interaction between the query and database local descriptors. We use the binary distilled variant of AMES with a universal model trained across varying local descriptor counts. The ensemble similarity between global and local features is

computed as a weighted combination, tuned via grid search.

ILIAS Baseline We also benchmark against the reranking strategy proposed in the ILIAS benchmark [14]. This method involves reranking a shortlist of images retrieved via global descriptors using dense feature correlation with ground-truth instance boxes. As this approach depends on densely sampled or region proposal-based local features, it tends to have higher memory and computation overhead.

Hyperparameter Search Since reranking approaches combine global and local similarities, hyperparameter tuning is critical. We perform a grid search over the following parameters to identify the best configuration:

- Number of reranked candidates: $[0, 100, 200, 400, 800, 1000]$
- Global-local balance weight λ : $[0.0, 0.1, 0.2, 0.3, 0.4, 0.5, 0.6, 0.7, 0.8, 0.9, 1.0]$
- Temperature scaling γ : $[0.0, 0.05, 0.1, 0.2, 0.3, 0.4, 0.5, 0.6, 0.7, 0.8, 0.9, 1.0]$

We report the performance using the best configuration selected from this grid for each method.

S5.2. Retrieval performance on ILIAS core set

We compare against two SOTA methods: DINOv2 w/ registers [4] from AMES [32], and SigLIP with linear adaptation [14] from ILIAS. As summarized in Table 6, Patchify achieves stronger performance than the fine-tuned baseline on both single-stage and reranking methods. This is aligned with the results on mini-ILIAS, which was reported in the main paper.

S5.3. LocScore on mini-ILIAS

As shown in Table 8, consistent with the earlier results, we observe the same trend: as mAP increases, LocScore increases as well.

S6. Product Quantization

To enable scalable retrieval with local features, we adopt Inverted File with Product Quantization (IVFPQ), a widely used technique that combines coarse clustering with quantization to allow efficient approximate nearest neighbor search with significantly reduced memory and latency overhead. To configure IVFPQ, we perform a grid search over the number of subvectors $m \in \{16, 32, 64\}$ and the number of clusters $nlist \in \{2048, 4096\}$, and select $m = 64$, $nlist = 4096$, and $nbins = 8$ based on retrieval performance.

Table 7 summarizes the impact of increasing patch granularity on database size before and after applying IVFPQ.

Table 7. Impact of multi-scale feature levels on storage size (MB) before and after applying product quantization. CR denotes the compression ratio. We observe that compression is scalable to high memory database.

Level (No. Patches)	INSTRE		ILIAS	
	Non-quant.	Quant (CR)	Non-quant.	Quant (CR)
L0 (1)	103.68	19.77 (5.24)	19.08	18.21 (1.05)
L1 (5)	518.42	27.41 (18.91)	95.41	19.62 (4.86)
L2 (14)	1420	44.61 (31.83)	267.15	22.78 (11.73)
L3 (30)	3040	71.71 (42.39)	572.46	28.41 (20.15)

As the number of patches increases from L0 to L3, uncompressed storage grows rapidly, by more than 29x on INSTRE and 30x on ILIAS. However, with IVFPQ, this increase is drastically reduced to just 3.6x and 1.6x, respectively. These results confirm that IVFPQ effectively scales to high-resolution patch representations, enabling practical deployment of patch-based retrieval with minimal memory overhead.

We investigate how the choice of training features affects PQ effectiveness. As summarized in Table 4, the highest performance is achieved when PQ is trained with features extracted from ground-truth bounding boxes (G.T.), which provide strong semantic alignment with the target instances. In contrast, using patches from intermediate configurations (e.g., L1 and L2) results in lower performance, possibly due to noisy or irrelevant background content in those features. Interestingly, PQ trained with global features (L0) outperforms L1 and L2, suggesting that lower-resolution but semantically focused representations may be more beneficial than ambiguous fine-grained features.

Qualitative examples in Figure S6 support this observation: G.T.-trained PQ accurately retrieves the correct instance under challenging conditions such as occlusion, scale change, and viewpoint variation, while PQ trained on L2 fails to distinguish between visually similar but incorrect instances. These findings highlight the importance of using informative training features for PQ optimization and offer valuable guidance for future work on compressed local feature retrieval.

S7. LocScore

This section provides extended analyses of the localization behavior measured by LocScore that were omitted from the main paper due to space limits. While the main paper introduced the metric and its motivation, here we investigate how different IoU criteria affect retrieval behavior and how localization quality varies across feature levels and model variants.

Figures S7 and S8 visualize the thresholded LocScore(δ) for multiple IoU thresholds on ILIAS-core and INSTRE. These results reveal that different models degrade at differ-



Figure S5. Images used to train PQ indices in each Patchify level and G.T. We can observe that features from G.T. are related to the instance, directly.

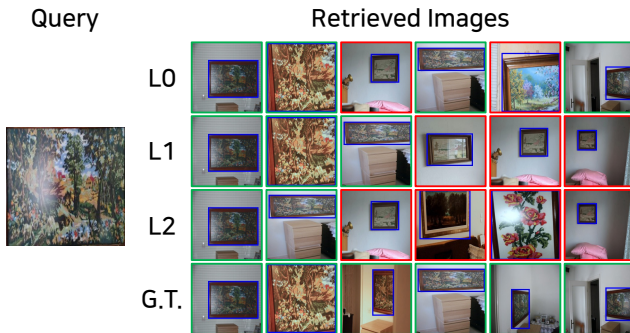


Figure S6. Qualitative retrieval results using different PQ training features at L3. PQ trained on G.T. finds the correct instance compared to others. Thus, we also consider the informative features when training PQ.

ent rates as the spatial criterion becomes stricter. For example, methods that rely on coarse global features show a rapid decline beyond $\delta=0.3$, whereas patch-based retrieval remains more stable up to $\delta=0.5$. This indicates that localization robustness is tightly linked to the granularity of visual evidence used by the model.

Figures 9 and 10 report the LocScore averaged across thresholds, providing a summary measure that reflects overall spatial reliability. This aggregated score smooths out threshold-specific fluctuations and highlights consistent performance trends that are not fully visible from single-threshold evaluations. In particular, models with strong mid-level representations maintain competitive scores across a wide range of δ , suggesting that localization

accuracy is distributed across multiple feature layers rather than dominated by a single level.

Figure 5 illustrates how different IoU criteria impact qualitative retrieval outcomes. Unlike the continuous variant, which reflects gradual changes in spatial alignment, thresholded LocScore(δ) exposes failure modes where retrieved patches partially overlap the target but fail to satisfy a strict IoU requirement. These cases highlight the sensitivity of certain models to small spatial displacements. The contrast between the two forms, therefore, helps to diagnose whether a model's failure stems from ranking errors (low IoU overall) or boundary precision (IoU slightly below δ).

Together, these supplementary results provide a more complete understanding of the spatial behavior of retrieval systems. They show how localization precision evolves under increasingly strict criteria, how robustness varies across feature hierarchies, and how different formulations of LocScore reveal distinct types of spatial failure.

Qualitative results of LocScore variants Figure S11a compares different localization strategies for the same query—Global, Patchify, Patchify with a sliding window (stride 0.25), and the Region Proposal variant. Improved localization accuracy leads to higher IoU, which subsequently improves both AP and LocScore. The Region Proposal method exhibits the best localization quality and obtains the highest scores.

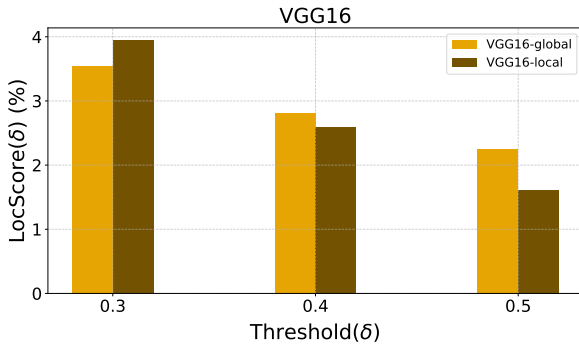
Figure S11b contrasts the continuous LocScore with its thresholded versions LocScore(δ) at different IoU thresholds. Although the continuous LocScore differs only by about 0.05 between the two rows, the thresholded scores change dramatically as δ increases, illustrating how sensitive LocScore(δ) is to the definition of acceptable localization quality.

Figure S11c mirrors the example in the main paper, highlighting the relationship between AP and LocScore. Even when AP is relatively high, LocScore can remain low if the predicted regions have poor overlap with the ground-truth boxes, showing that improving LocScore requires not only strong ranking (high AP) but also accurate localization with high IoU.

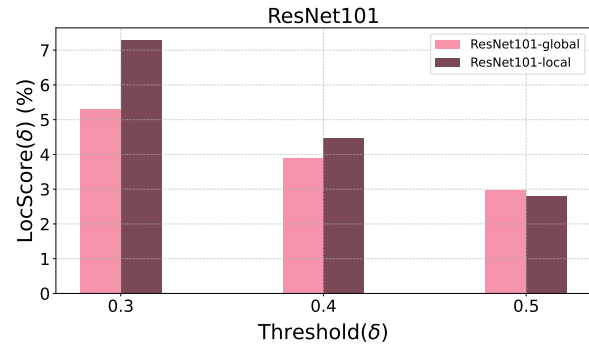
Limitations. LocScore is tightly coupled with AP because it multiplies rank-based contribution by IoU, so the score can be overly driven by the localization quality of a few top-ranked positives while good localization at lower ranks has little influence. The thresholded variant partly alleviates this by enforcing a minimum IoU, but it introduces subjectivity since the notion of “good localization” depends on a human-chosen threshold. To reduce this ambiguity, we additionally report a mean version of LocScore and present both the continuous and thresholded variants side by side. We added this discussion to the supplementary.

Model	Level	mAP@1k	LocScore (cont.)	mLocScore	LocScore (δ)
SigLIP	L0 (Global)	0.2041	6.59	5.60	$\delta=0.3 : 7.55$
					$\delta=0.4 : 5.38$
					$\delta=0.5 : 3.86$
					$\delta=0.3 : 12.56$
SigLIP	L1	0.2968	10.08	8.92	$\delta=0.4 : 8.37$
					$\delta=0.5 : 5.83$
					$\delta=0.3 : 24.78$
SigLIP	L2	0.5027	18.11	16.21	$\delta=0.4 : 15.43$
					$\delta=0.5 : 8.41$
					$\delta=0.3 : 10.58$
SigLIP	L3	0.2608	8.81	7.55	$\delta=0.4 : 7.32$
					$\delta=0.5 : 4.76$
SigLIP[†]	L0 (Global)	0.3386	9.59	7.40	$\delta=0.3 : 10.39$
					$\delta=0.4 : 7.11$
					$\delta=0.5 : 4.72$
SigLIP[†]	L1	0.3655	11.08	8.99	$\delta=0.3 : 12.69$
					$\delta=0.4 : 8.50$
					$\delta=0.5 : 5.78$
SigLIP[†]	L2	0.3924	12.29	9.92	$\delta=0.3 : 14.22$
					$\delta=0.4 : 9.46$
					$\delta=0.5 : 6.08$
SigLIP[†]	L3	0.4048	12.82	10.33	$\delta=0.3 : 15.04$
					$\delta=0.4 : 9.77$
					$\delta=0.5 : 6.19$
DINOv3	L0 (Global)	0.2180	8.02	7.40	$\delta=0.3 : 9.55$
					$\delta=0.4 : 7.26$
					$\delta=0.5 : 5.39$
DINOv3	L1	0.3147	11.48	10.25	$\delta=0.3 : 14.22$
					$\delta=0.4 : 9.68$
					$\delta=0.5 : 6.86$
DINOv3	L2	0.3954	15.71	15.31	$\delta=0.3 : 22.33$
					$\delta=0.4 : 14.53$
					$\delta=0.5 : 9.08$
DINOv3	L3	0.4298	17.05	16.44	$\delta=0.3 : 24.72$
					$\delta=0.4 : 15.32$
					$\delta=0.5 : 9.29$

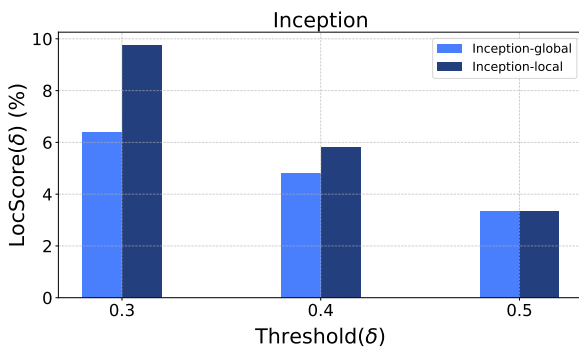
Table 8. Quantitative results on mini-ILIAS with mAP@1k and LocScore variants. A dagger ([†]) denotes the linear adaptation baseline from ILIAS; δ is the IoU threshold for the thresholded LocScore.



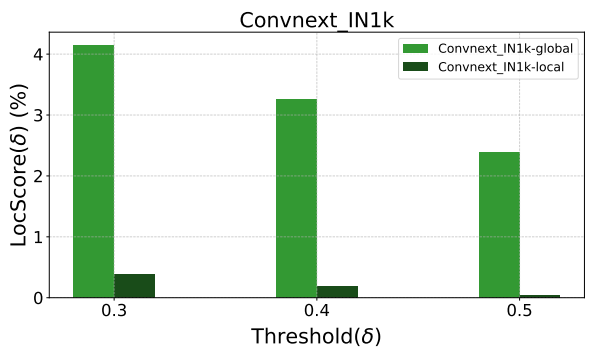
(a) VGG16



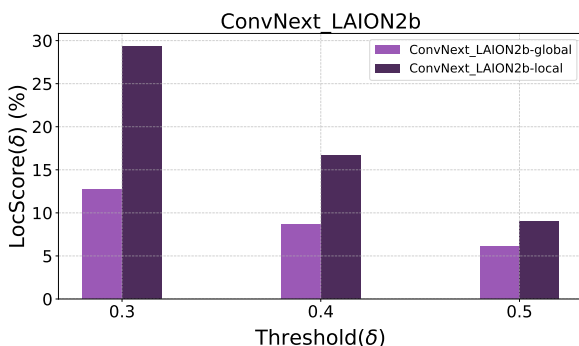
(b) ResNet



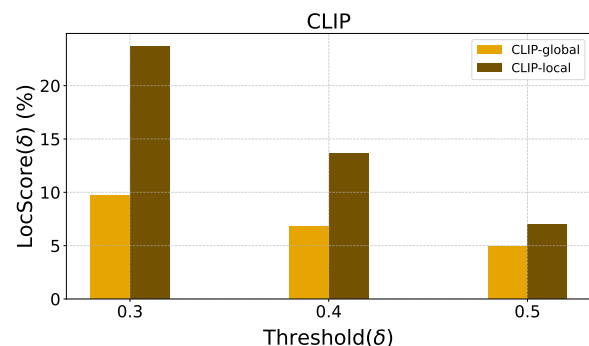
(c) Inception



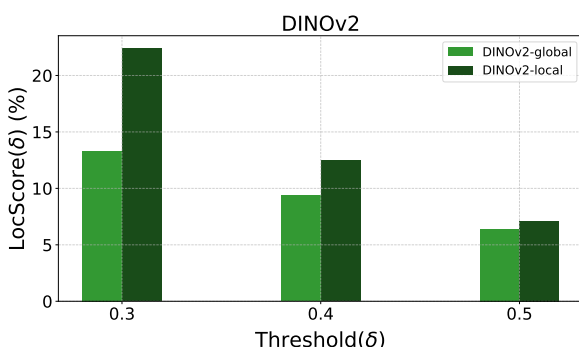
(d) ConvNext-IN1k



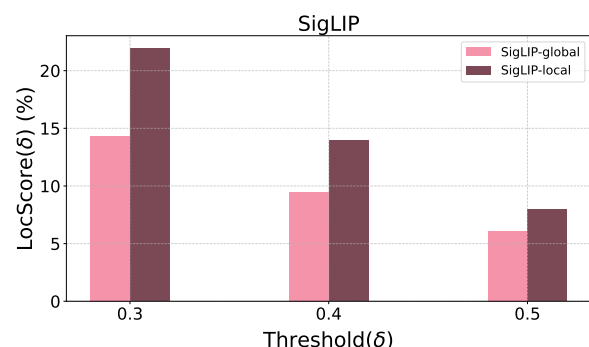
(e) ConvNext-LAION2b



(f) CLIP

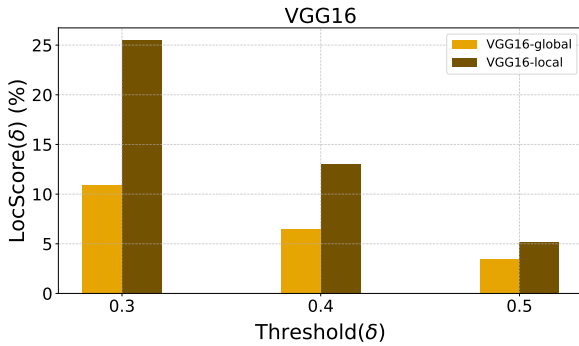


(g) DINOv2

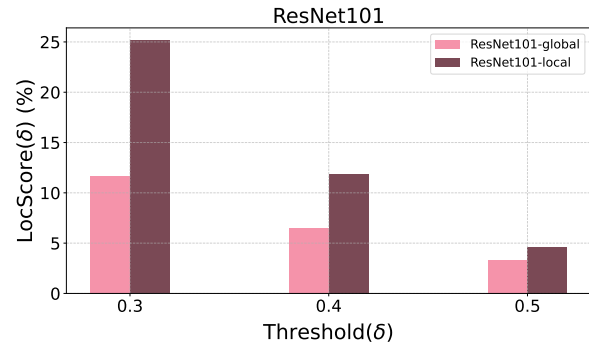


(h) SigLIP

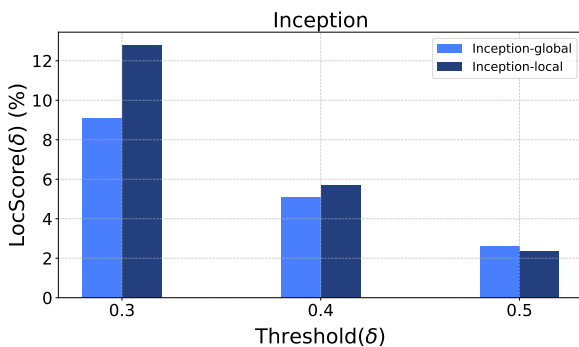
Figure S7. LocScore(δ) visualizations across threshold $\delta = 0.3, 0.4, 0.5$ of CNN-based and Transformer-based models on ILIAS.



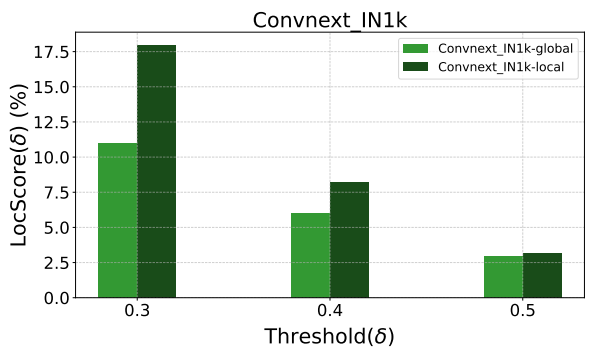
(a) VGG16



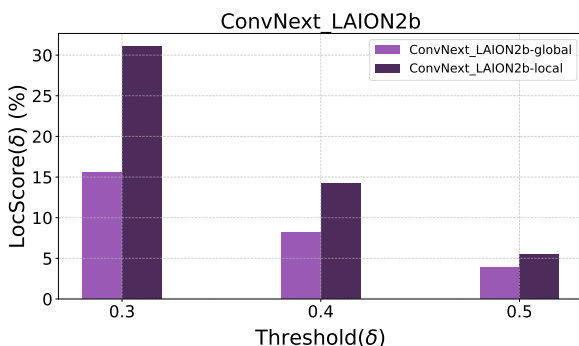
(b) ResNet



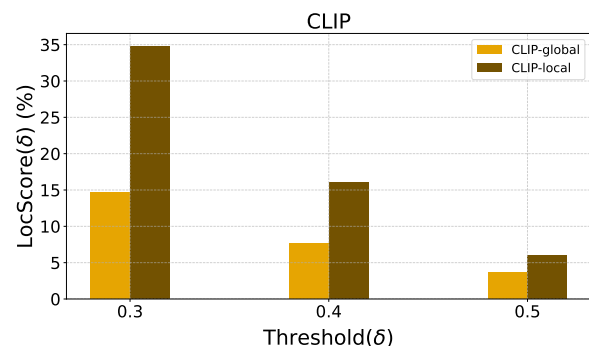
(c) Inception



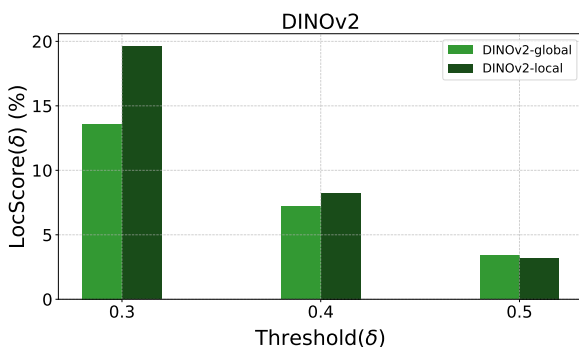
(d) ConvNext-IN1k



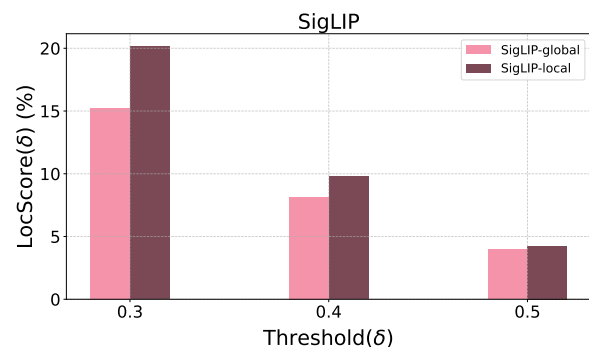
(e) ConvNext-LAION2b



(f) CLIP



(g) DINOv2



(h) SigLIP

Figure S8. LocScore(δ) visualizations across threshold $\delta = 0.3, 0.4, 0.5$ of CNN-based and Transformer-based models on INSTRE.

model	Level	INSTRE				ILIAS			
		mAP	LocScore	mLocScore	LocScore(δ)	mAP	LocScore	mLocScore	LocScore(δ)
VGG16	L0	26.690	8.842	6.960	$\delta=0.3 : 10.928$	5.864	2.625	2.866	$\delta=0.3 : 3.540$
					$\delta=0.4 : 6.526$				$\delta=0.4 : 2.814$
					$\delta=0.5 : 3.426$				$\delta=0.5 : 2.245$
	L1	39.859	13.697	9.453	$\delta=0.3 : 16.400$	7.399	2.718	2.468	$\delta=0.3 : 3.359$
					$\delta=0.4 : 8.295$				$\delta=0.4 : 2.396$
					$\delta=0.5 : 3.665$				$\delta=0.5 : 1.649$
	L2	51.186	19.189	14.331	$\delta=0.3 : 24.852$	8.485	2.978	2.728	$\delta=0.3 : 3.852$
					$\delta=0.4 : 12.865$				$\delta=0.4 : 2.614$
					$\delta=0.5 : 5.277$				$\delta=0.5 : 1.719$
	L3	53.562	19.813	14.561	$\delta=0.3 : 25.461$	8.764	3.030	2.716	$\delta=0.3 : 3.941$
					$\delta=0.4 : 12.999$				$\delta=0.4 : 2.595$
					$\delta=0.5 : 5.223$				$\delta=0.5 : 1.613$
ResNet101	L0	36.288	10.763	7.147	$\delta=0.3 : 11.643$	10.396	4.111	4.064	$\delta=0.3 : 5.296$
					$\delta=0.4 : 6.505$				$\delta=0.4 : 3.908$
					$\delta=0.5 : 3.293$				$\delta=0.5 : 2.989$
	L1	48.757	15.892	9.725	$\delta=0.3 : 17.410$	13.300	4.941	4.367	$\delta=0.3 : 6.110$
					$\delta=0.4 : 8.259$				$\delta=0.4 : 4.158$
					$\delta=0.5 : 3.504$				$\delta=0.5 : 2.832$
	L2	58.588	21.058	14.150	$\delta=0.3 : 25.269$	15.410	5.573	4.969	$\delta=0.3 : 7.309$
					$\delta=0.4 : 12.284$				$\delta=0.4 : 4.640$
					$\delta=0.5 : 4.896$				$\delta=0.5 : 2.959$
	L3	61.382	21.558	13.893	$\delta=0.3 : 25.138$	16.193	5.625	4.853	$\delta=0.3 : 7.276$
					$\delta=0.4 : 11.894$				$\delta=0.4 : 4.467$
					$\delta=0.5 : 4.646$				$\delta=0.5 : 2.815$
Inception	L0	27.943	8.435	5.585	$\delta=0.3 : 9.066$	14.624	5.260	4.859	$\delta=0.3 : 6.410$
					$\delta=0.4 : 5.105$				$\delta=0.4 : 4.812$
					$\delta=0.5 : 2.584$				$\delta=0.5 : 3.355$
	L1	34.592	10.866	6.325	$\delta=0.3 : 11.091$	18.026	6.418	5.545	$\delta=0.3 : 7.807$
					$\delta=0.4 : 5.464$				$\delta=0.4 : 5.275$
					$\delta=0.5 : 2.422$				$\delta=0.5 : 3.552$
	L2	42.077	13.755	7.676	$\delta=0.3 : 13.787$	21.385	7.484	6.557	$\delta=0.3 : 9.831$
					$\delta=0.4 : 6.513$				$\delta=0.4 : 6.187$
					$\delta=0.5 : 2.728$				$\delta=0.5 : 3.652$
	L3	45.822	14.112	6.952	$\delta=0.3 : 12.808$	23.631	7.757	6.310	$\delta=0.3 : 9.769$
					$\delta=0.4 : 5.698$				$\delta=0.4 : 5.810$
					$\delta=0.5 : 2.350$				$\delta=0.5 : 3.350$
ConvNext.IN1k	L0	38.972	11.006	6.649	$\delta=0.3 : 10.981$	8.606	3.253	3.266	$\delta=0.3 : 4.153$
					$\delta=0.4 : 5.993$				$\delta=0.4 : 3.253$
					$\delta=0.5 : 2.974$				$\delta=0.5 : 2.394$
	L1	47.535	14.549	7.727	$\delta=0.3 : 13.879$	2.517	0.705	0.505	$\delta=0.3 : 0.820$
					$\delta=0.4 : 6.535$				$\delta=0.4 : 0.451$
					$\delta=0.5 : 2.768$				$\delta=0.5 : 0.243$
	L2	54.045	17.939	10.173	$\delta=0.3 : 18.403$	2.232	0.549	0.355	$\delta=0.3 : 0.658$
					$\delta=0.4 : 8.663$				$\delta=0.4 : 0.312$
					$\delta=0.5 : 3.452$				$\delta=0.5 : 0.096$
	L3	56.254	18.163	9.793	$\delta=0.3 : 17.984$	1.902	0.421	0.206	$\delta=0.3 : 0.392$
					$\delta=0.4 : 8.203$				$\delta=0.4 : 0.187$
					$\delta=0.5 : 3.193$				$\delta=0.5 : 0.041$

Table 9. Quantitative results with mAP and LocScore under various backbones.

model	Level	INSTRE				ILIAS			
		mAP	LocScore	mLocScore	LocScore(δ)	mAP	LocScore	mLocScore	LocScore(δ)
ConvNext_LAION2b	L0	77.949	19.005	9.171	$\delta=0.3 : 15.531$	41.253	11.886	9.156	$\delta=0.3 : 12.752$
					$\delta=0.4 : 8.135$				$\delta=0.4 : 8.672$
					$\delta=0.5 : 3.847$				$\delta=0.5 : 6.043$
	L1	86.710	24.872	11.977	$\delta=0.3 : 21.397$	50.754	16.078	12.302	$\delta=0.3 : 19.025$
					$\delta=0.4 : 10.228$				$\delta=0.4 : 11.002$
					$\delta=0.5 : 4.306$				$\delta=0.5 : 6.880$
	L2	91.524	30.159	16.453	$\delta=0.3 : 30.010$	60.215	20.789	17.296	$\delta=0.3 : 27.039$
					$\delta=0.4 : 13.943$				$\delta=0.4 : 16.130$
					$\delta=0.5 : 5.407$				$\delta=0.5 : 8.719$
	L3	92.870	30.936	16.953	$\delta=0.3 : 31.109$	64.441	22.221	18.333	$\delta=0.3 : 29.363$
					$\delta=0.4 : 14.263$				$\delta=0.4 : 16.688$
					$\delta=0.5 : 5.488$				$\delta=0.5 : 8.948$
DINOv2	L0	57.701	15.074	8.063	$\delta=0.3 : 13.593$	40.557	12.181	9.698	$\delta=0.3 : 13.332$
					$\delta=0.4 : 7.185$				$\delta=0.4 : 9.374$
					$\delta=0.5 : 3.411$				$\delta=0.5 : 6.386$
	L1	64.621	18.738	8.781	$\delta=0.3 : 16.078$	46.825	14.932	11.476	$\delta=0.3 : 16.526$
					$\delta=0.4 : 7.285$				$\delta=0.4 : 10.594$
					$\delta=0.5 : 2.980$				$\delta=0.5 : 7.309$
	L2	69.978	22.183	11.065	$\delta=0.3 : 20.583$	52.918	17.371	13.460	$\delta=0.3 : 20.722$
					$\delta=0.4 : 9.056$				$\delta=0.4 : 12.330$
					$\delta=0.5 : 3.556$				$\delta=0.5 : 7.328$
	L3	72.543	22.216	10.343	$\delta=0.3 : 19.611$	57.515	18.492	13.999	$\delta=0.3 : 22.401$
					$\delta=0.4 : 8.233$				$\delta=0.4 : 12.485$
					$\delta=0.5 : 3.184$				$\delta=0.5 : 7.110$
OpenCLIP	L0	73.837	18.107	8.638	$\delta=0.3 : 14.594$	31.598	9.183	7.143	$\delta=0.3 : 9.696$
					$\delta=0.4 : 7.659$				$\delta=0.4 : 6.827$
					$\delta=0.5 : 3.660$				$\delta=0.5 : 4.904$
	L1	78.812	23.034	11.454	$\delta=0.3 : 21.196$	39.819	12.170	9.302	$\delta=0.3 : 14.501$
					$\delta=0.4 : 9.428$				$\delta=0.4 : 8.278$
					$\delta=0.5 : 3.737$				$\delta=0.5 : 5.129$
	L2	85.594	29.556	18.428	$\delta=0.3 : 33.733$	48.878	16.425	14.039	$\delta=0.3 : 21.976$
					$\delta=0.4 : 15.674$				$\delta=0.4 : 13.256$
					$\delta=0.5 : 5.877$				$\delta=0.5 : 6.885$
	L3	87.565	30.370	18.936	$\delta=0.3 : 34.804$	53.351	17.945	14.767	$\delta=0.3 : 23.706$
					$\delta=0.4 : 16.053$				$\delta=0.4 : 13.598$
					$\delta=0.5 : 5.953$				$\delta=0.5 : 6.998$
SigLIP	L0	78.483	18.918	9.120	$\delta=0.3 : 15.261$	55.029	14.305	9.969	$\delta=0.3 : 14.345$
					$\delta=0.4 : 8.135$				$\delta=0.4 : 9.469$
					$\delta=0.5 : 3.965$				$\delta=0.5 : 6.095$
	L1	83.056	21.719	10.335	$\delta=0.3 : 17.815$	59.449	16.631	11.911	$\delta=0.3 : 17.504$
					$\delta=0.4 : 9.037$				$\delta=0.4 : 11.195$
					$\delta=0.5 : 4.154$				$\delta=0.5 : 7.033$
	L2	85.965	23.888	11.526	$\delta=0.3 : 20.255$	63.319	18.842	13.888	$\delta=0.3 : 20.688$
					$\delta=0.4 : 9.963$				$\delta=0.4 : 13.368$
					$\delta=0.5 : 4.360$				$\delta=0.5 : 7.607$
	L3	87.015	24.285	11.397	$\delta=0.3 : 20.151$	65.165	19.745	14.613	$\delta=0.3 : 21.933$
					$\delta=0.4 : 9.777$				$\delta=0.4 : 13.933$
					$\delta=0.5 : 4.264$				$\delta=0.5 : 7.974$

Table 10. Quantitative results with mAP and LocScore under various backbones.

S8. Qualitative Results



Figure S9. Qualitative results of Global and Patchify on ILIAS

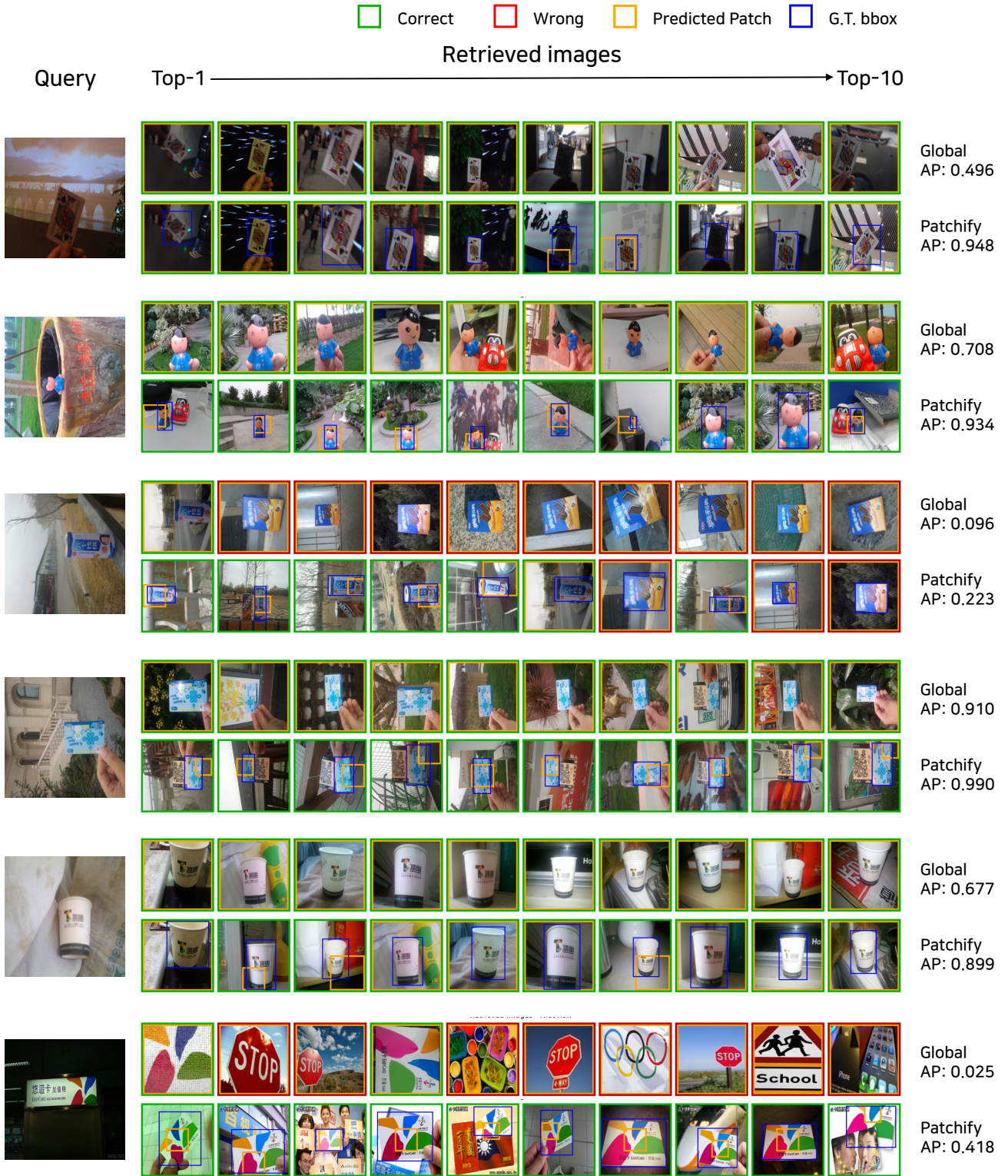
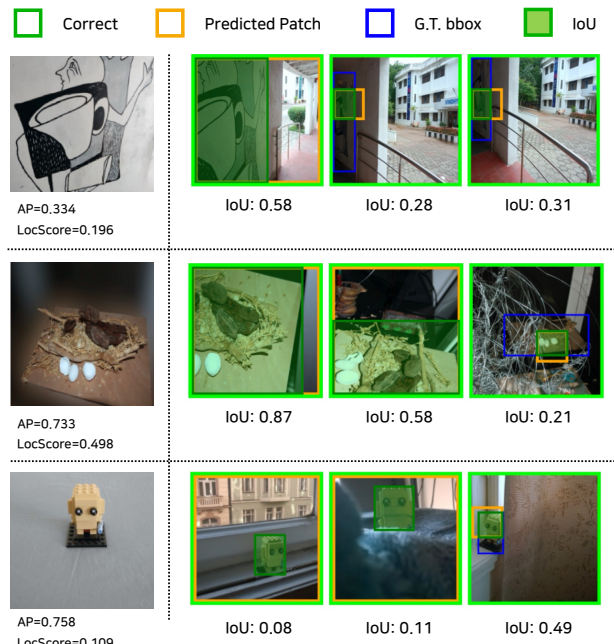
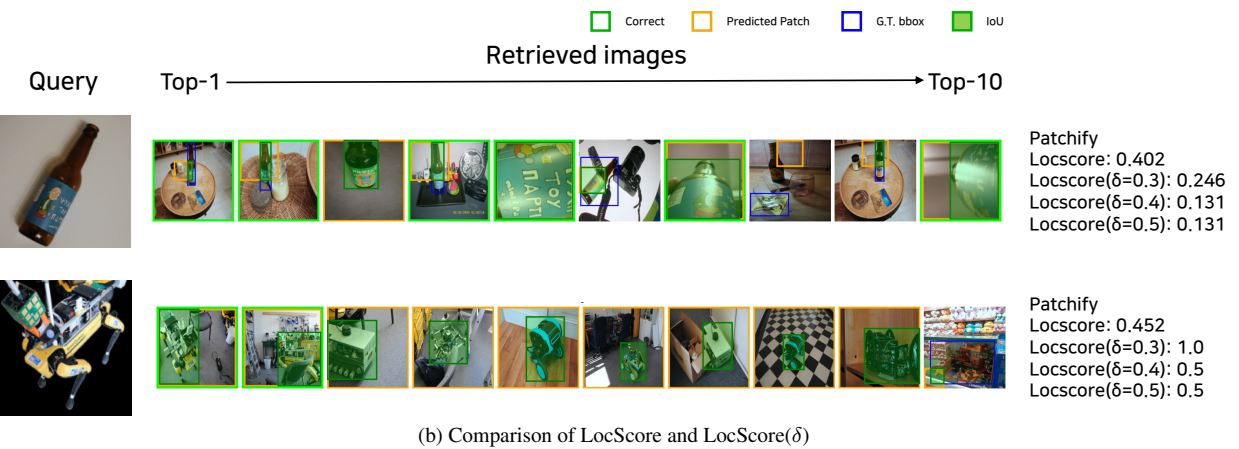
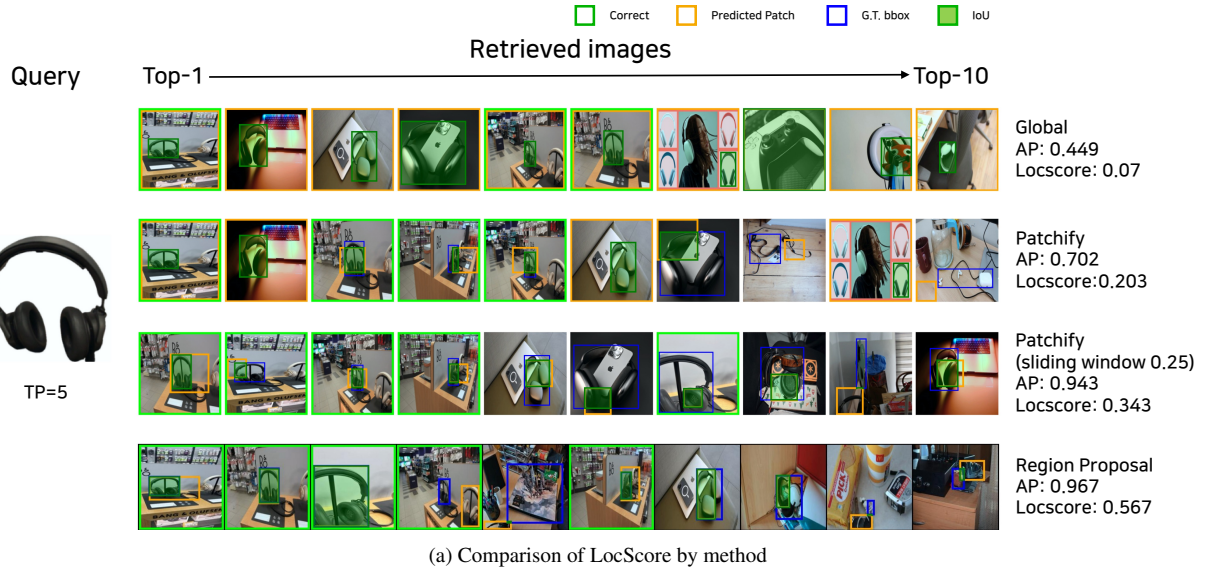


Figure S10. Qualitative results of Global and Patchify on INSTRE



(c) Comparison of AP and LocScore

Figure S11. Qualitative results of LocScore variants.